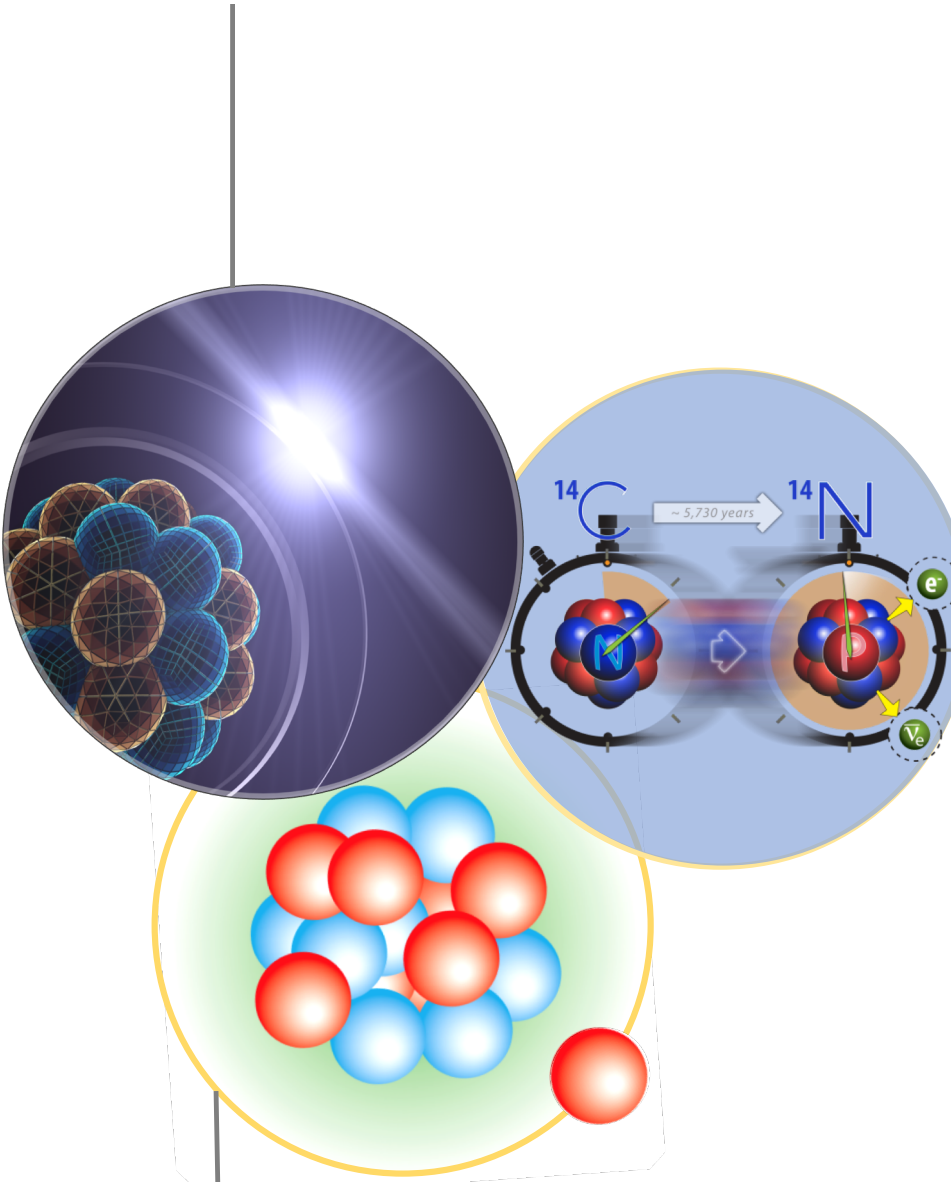


Modern Nuclear Theory & Neutron Skins

Gaute Hagen
Oak Ridge National Laboratory

Precision Tests with neutral-current coherent interactions with nuclei

MITP workshop, May 25th, 2022

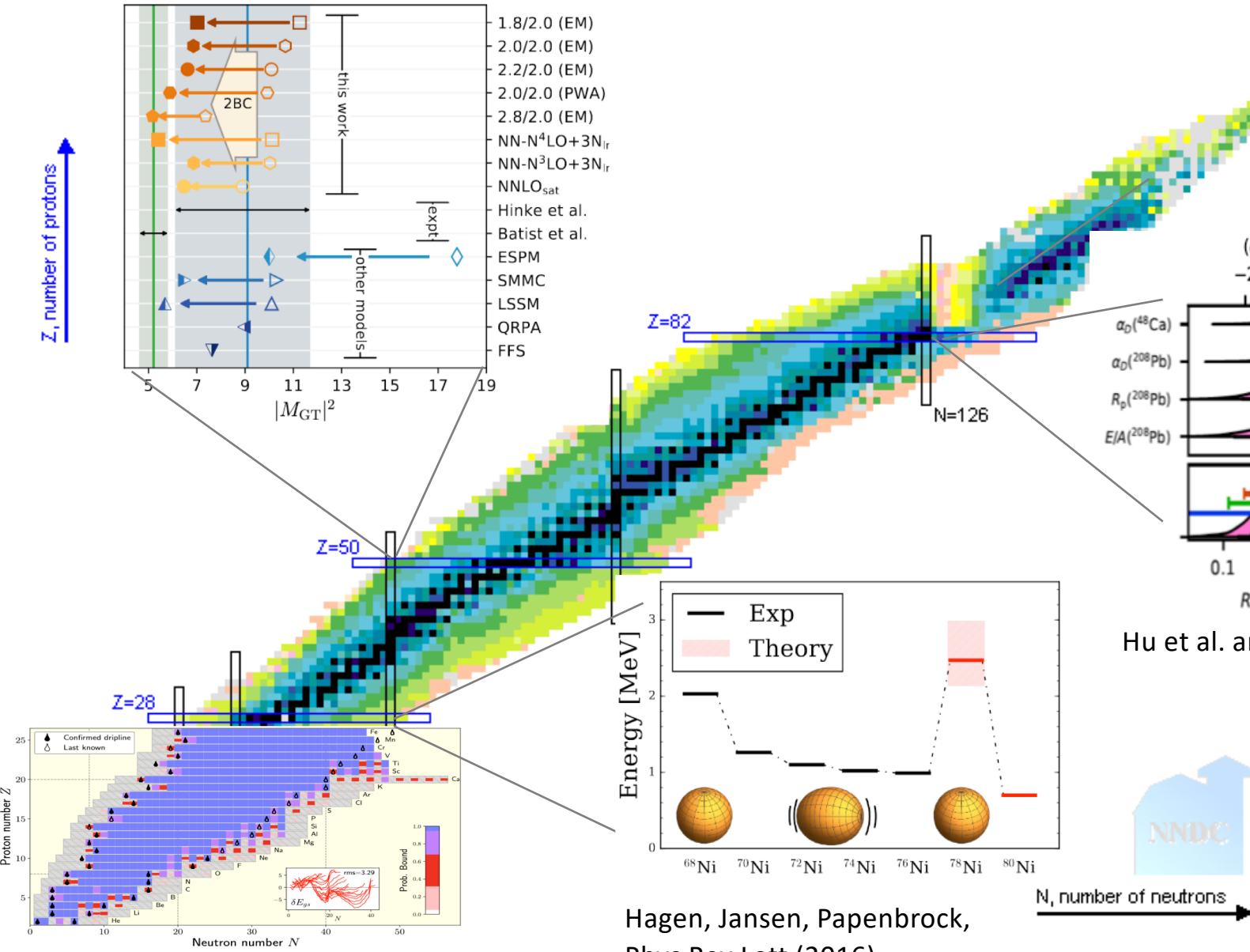


Collaborators

- @ ORNL / UTK: **B. Acharya**, G. R. Jansen, T. Morris, **Z. H. Sun**, T. Papenbrock
- @ ANL: **S. R. Stroberg**
- @ CEA/Saclay: T. Duguet
- @ Chalmers: A. Ekström, C. Forssén, **W. G. Jiang**
- @ Mainz: **F. Bonaiti**, S. Bacca, **J. E. Sobczyk**
- @ MSU: W. Nazarewicz
- @ LANL: **S. Novario**, S. Gandolfi, **D. Lonardoni**
- @ LLNL: K. Wendt, S. Quaglioni
- @ TRIUMF: **Baishun Hu**, **P. Gysbers**, J. Holt, P. Navratil
- @ TU Darmstadt: K. Hebeler, **T. Miyagi**, A. Schwenk, **A. Tichai**

The Hamiltonian knows best

Gysbers et al, Nat Phys (2019)



Stroberg et al, Phys Rev Lett (2021)

Hagen, Jansen, Papenbrock,
Phys Rev Lett (2016)

Hu et al. arXiv:2112.01125 (2022)

- An “ab initio revolution” is changing how we compute atomic nuclei
- What was long believed to be the exclusive domain of nuclear energy density functionals, is becoming accessible by Hamiltonians
 - Link nuclear structure to forces between few nucleons
 - Compute bulk properties (radii, BEs), spectra, and transitions
 - Perform symmetry projection
 - Ideas from EFT and the RG, and algorithms with an affordable scaling are paving the way

Coupled-cluster method (CCSD approximation)

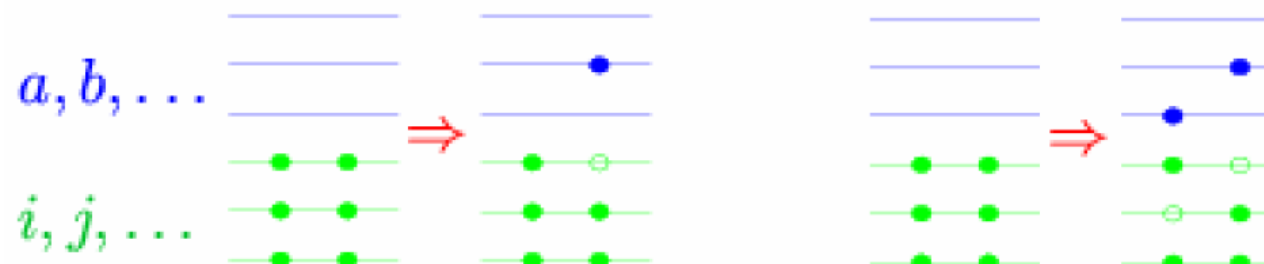
$$\Psi = e^T |\Phi\rangle$$

$$T = T_1 + T_2 + \dots$$

$$T_1 = \sum_{ia} t_i^a a_a^\dagger a_i \quad T_2 = \frac{1}{4} \sum_{ijab} t_{ij}^{ab} a_a^\dagger a_b^\dagger a_j a_i$$

- ☺ Scales gently (polynomial) with increasing system size
- ☺ Truncation is only approximation
- ☺ A lot of freedom in the choice of reference state (spherical, deformed, pairing,...)

Correlations are *exponentiated* 1p-1h and 2p-2h excitations. Part of Ap-Ah excitations included!



Coupled cluster equations

$$E = \langle \Phi | \bar{H} | \Phi \rangle$$

$$0 = \langle \Phi_i^a | \bar{H} | \Phi \rangle$$

$$0 = \langle \Phi_{ij}^{ab} | \bar{H} | \Phi \rangle$$

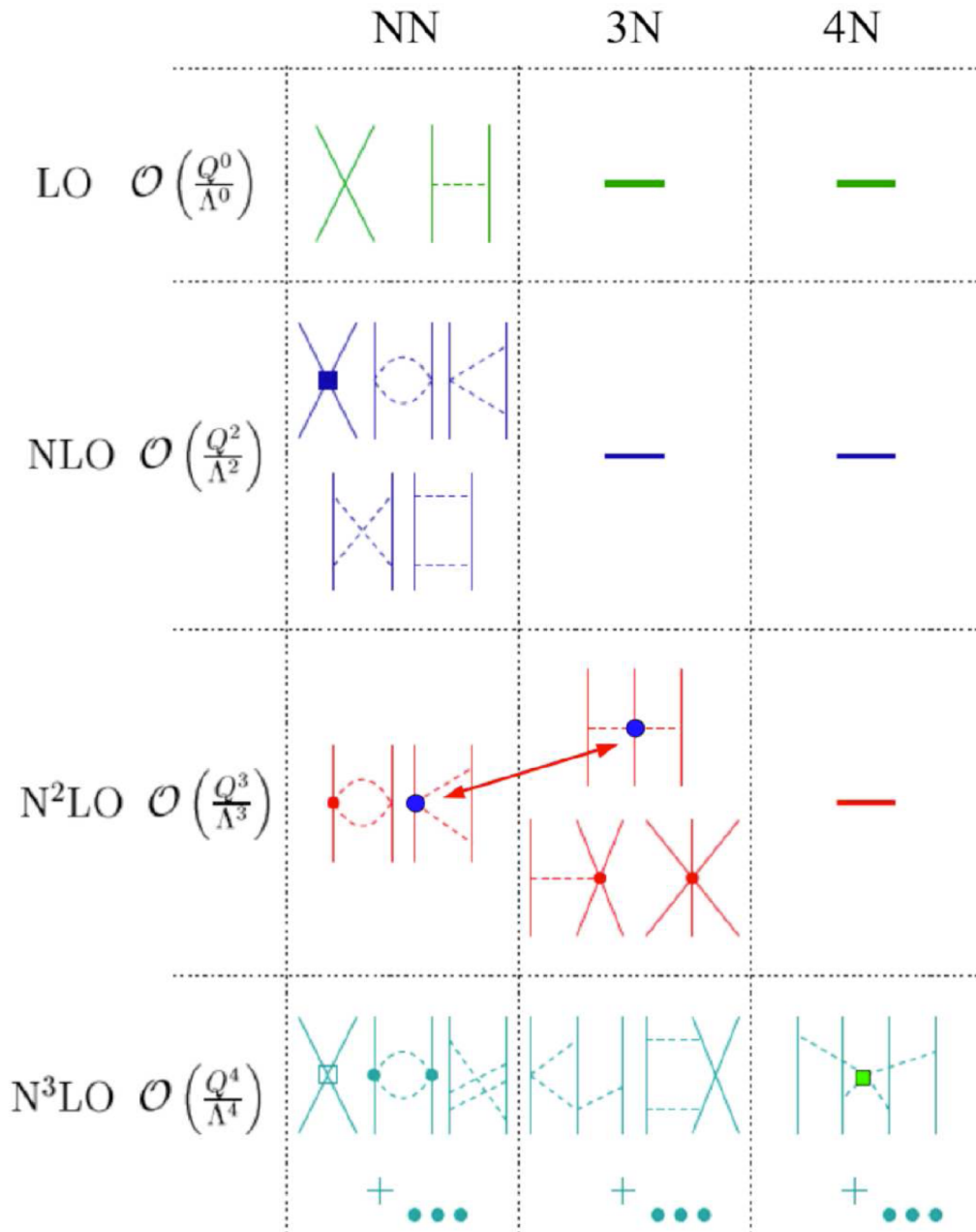
Alternative view: CCSD generates similarity transformed Hamiltonian with no 1p-1h and no 2p-2h excitations.

Normal-ordering effectively reduces the A-body to a few-body problem

$$\bar{H} \equiv e^{-T} H e^T = (H e^T)_c = \left(H + H T_1 + H T_2 + \frac{1}{2} H T_1^2 + \dots \right)_c$$

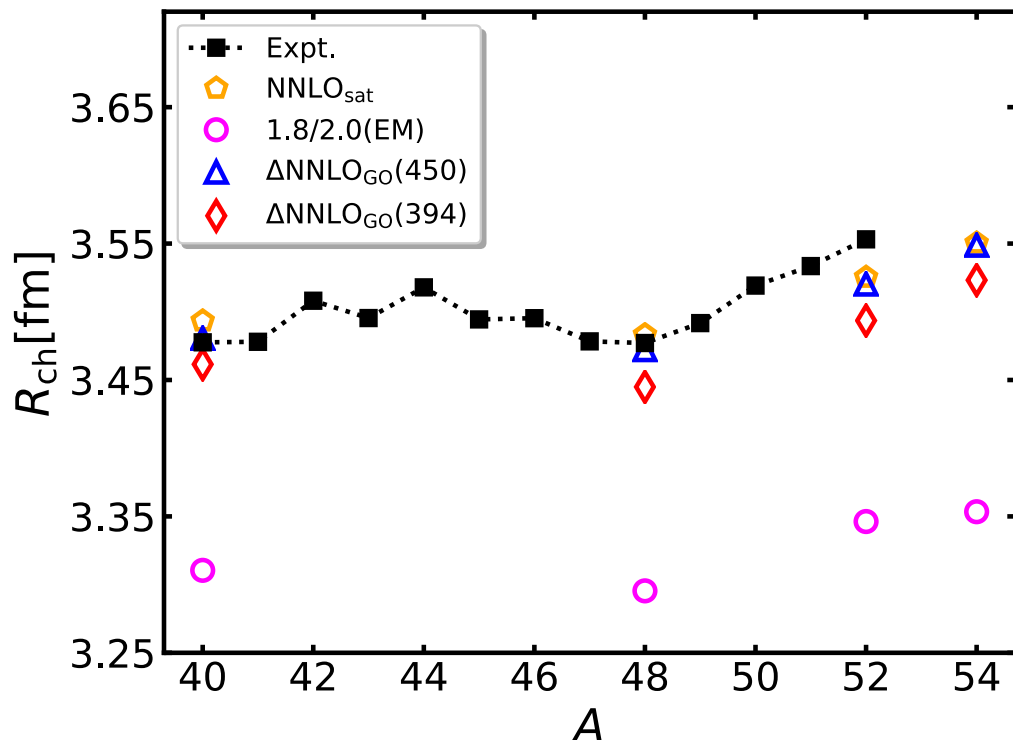
Nuclear forces from chiral effective field theory

[Weinberg; van Kolck; Epelbaum *et al.*; Entem & Machleidt; ...]



- Developing higher orders and higher rank (3NF, 4NF) [Epelbaum 2006; Bernard et al 2007; Krebs et al 2012; Hebeler et al 2015; Entem et al 2017, Reinert et al 2017...]
- Propagation of uncertainties on the horizon [Navarro Perez 2014, Carlsson et al 2015, Ekström & Hagen 2019, Drischler et al 2020]
- Different optimization protocols [Ekström et al 2013, Carlsson et al 2016]
- Improved understanding/handling via SRG [Bogner et al 2003; Bogner et al 2007]
- local / semi-local / non-local formulations [Epelbaum et al 2015, Gezerlis et al 2013/2014, Binder et al 2018]
- Chiral EFT's with explicit Delta isobars [Krebs et al 2018, Piarulli et al 2017, Ekström et al 2017, Jiang et al (2020)]

Some chiral potentials (models) work better than others



NNLO_{sat}: Accurate radii and BEs

Simultaneous optimization of NN and 3NFs

Include radii and BEs of 3H , $^{3,4}He$, ^{14}C , ^{16}O in the optimization

Harder interaction: difficult to converge beyond ^{56}Ni

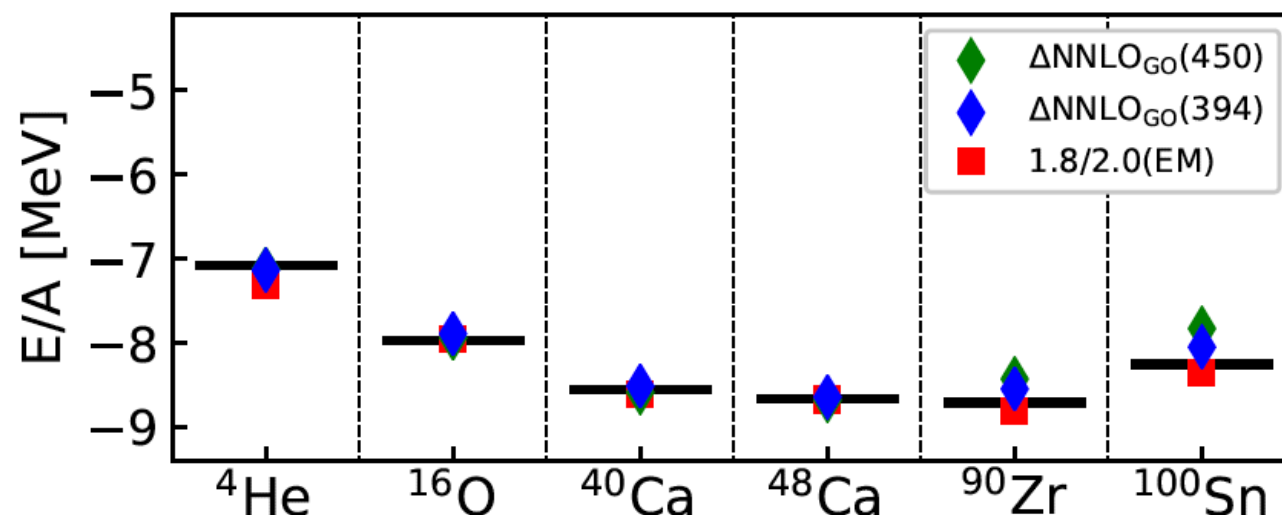
A. Ekström *et al*, Phys. Rev. C **91**, 051301(R) (2015)

Δ NNLO_{GO}: Accurate radii, BEs, and symmetry energy

Chiral EFT with explicit delta isobars

Include charge radii and binding energies of 3H , $^{3,4}He$, and nuclear matter saturation in the optimization

W. G. Jiang, *et al.*, Phys. Rev. C **102**, 054301 (2020)



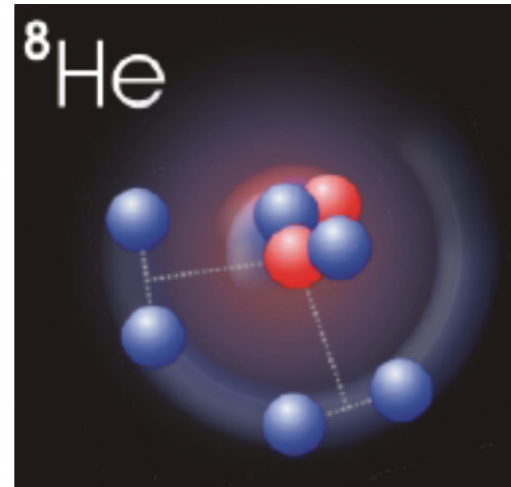
1.8/2.0(EM): Accurate BEs and spectra

Soft interaction: SRG N3LO from Entem & Machleidt with 3NF at NNLO from chiral EFT

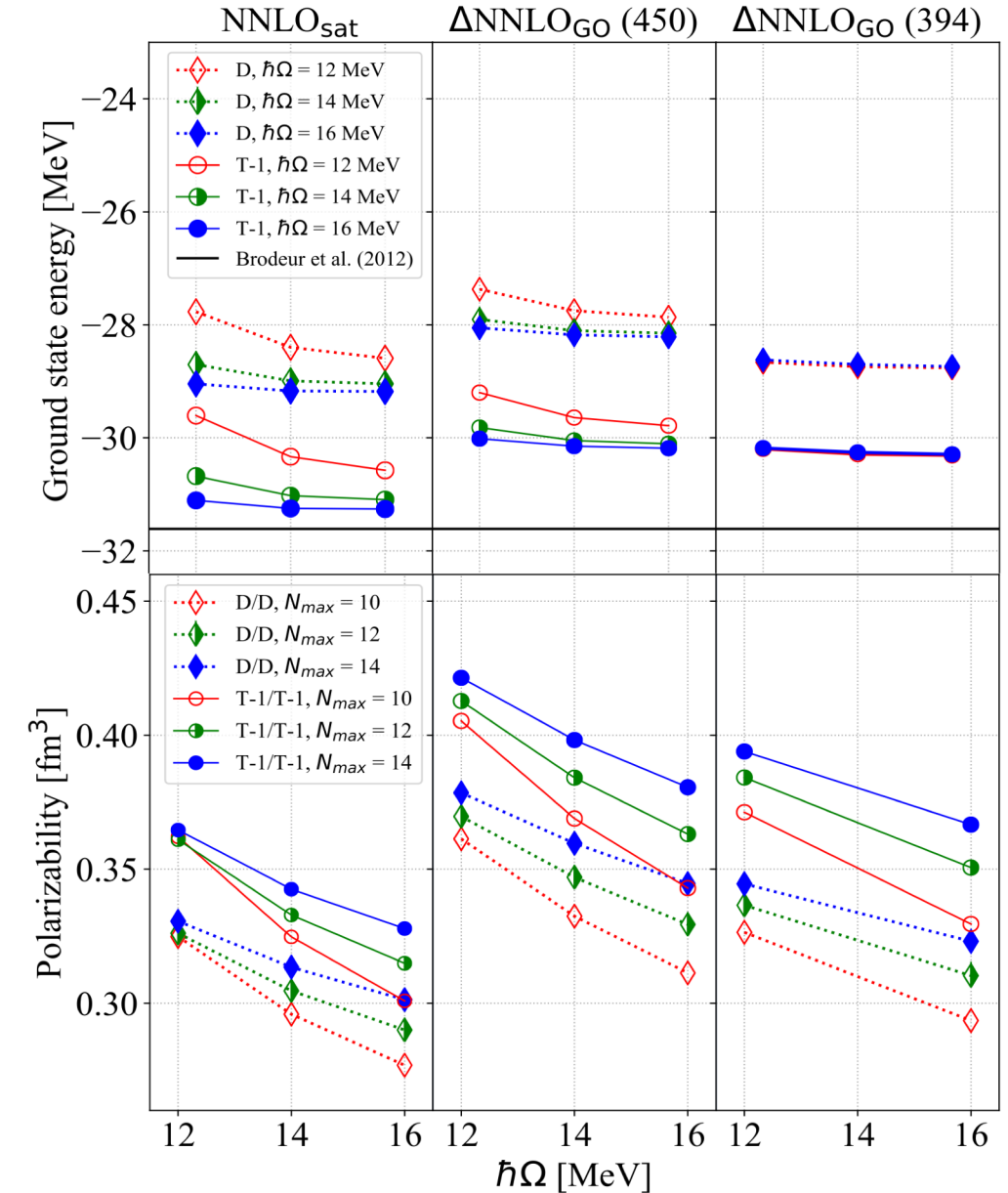
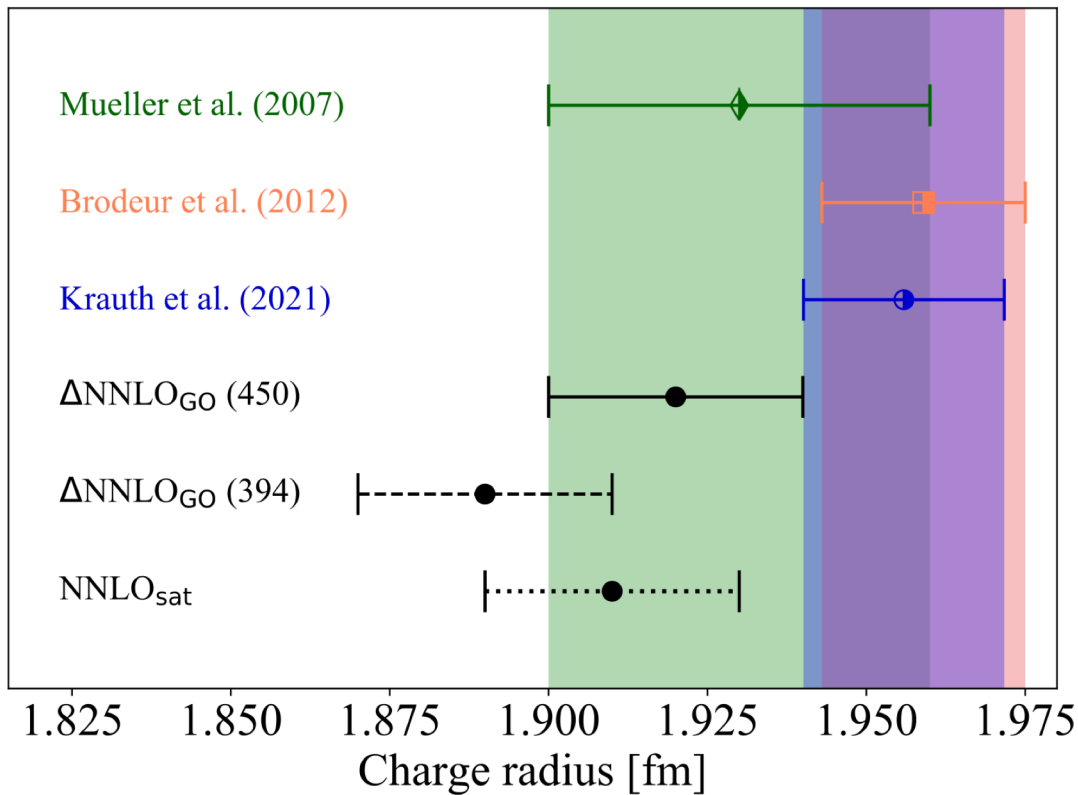
K. Hebeler *et al* PRC (2011).

T. Morris *et al*, PRL (2018).

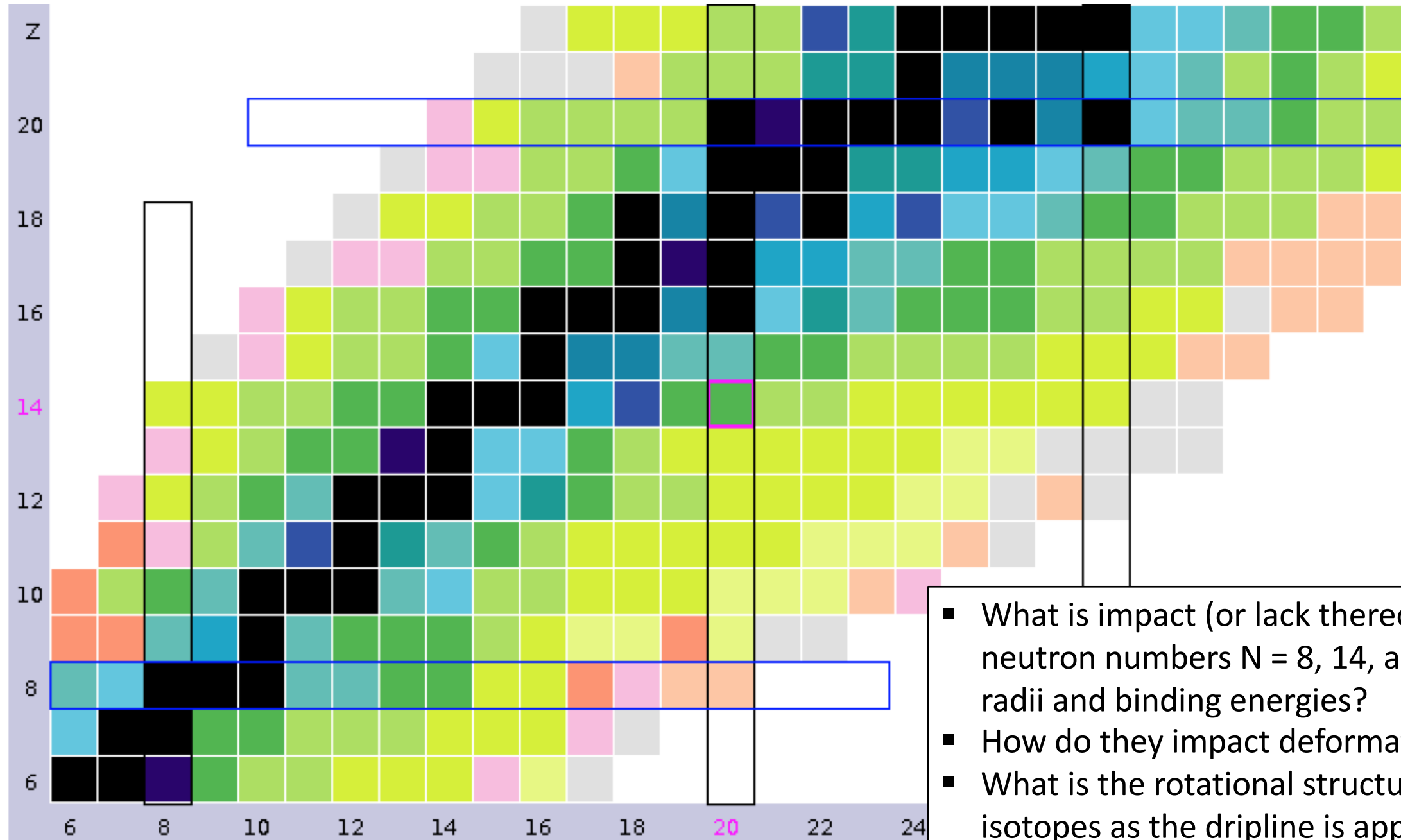
Charge radius and dipole polarizability of ${}^8\text{He}$



Francesca Bonaiti, Sonia Bacca, Gaute Hagen, Phys. Rev. C 105, 034313 (2022)

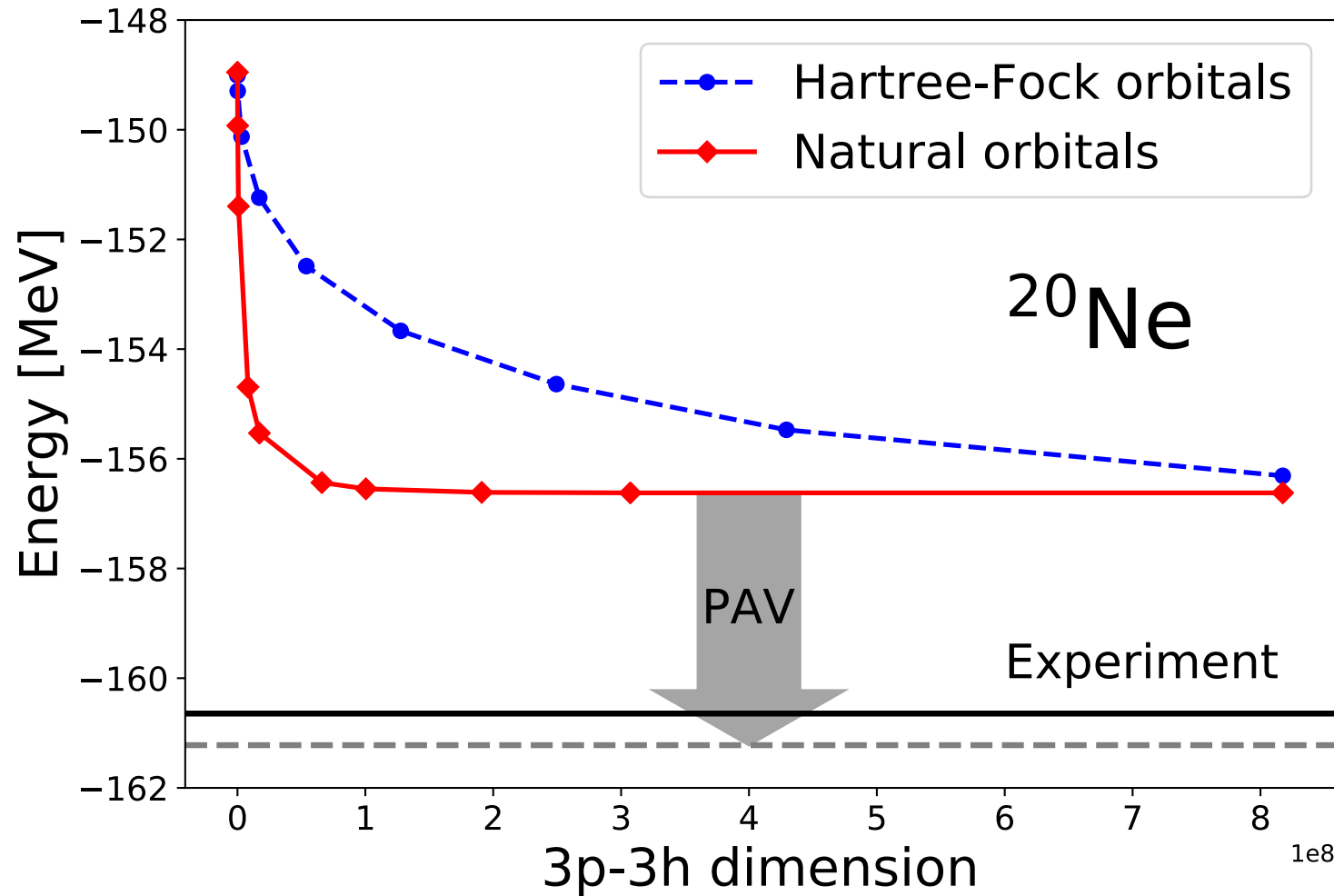


Towards island of inversion with ab initio methods



- What is impact (or lack thereof) of the “magic” neutron numbers $N = 8, 14$, and 20 on charge radii and binding energies?
- How do they impact deformation past $N = 20$?
- What is the rotational structure of neutron-rich isotopes as the dripline is approached?

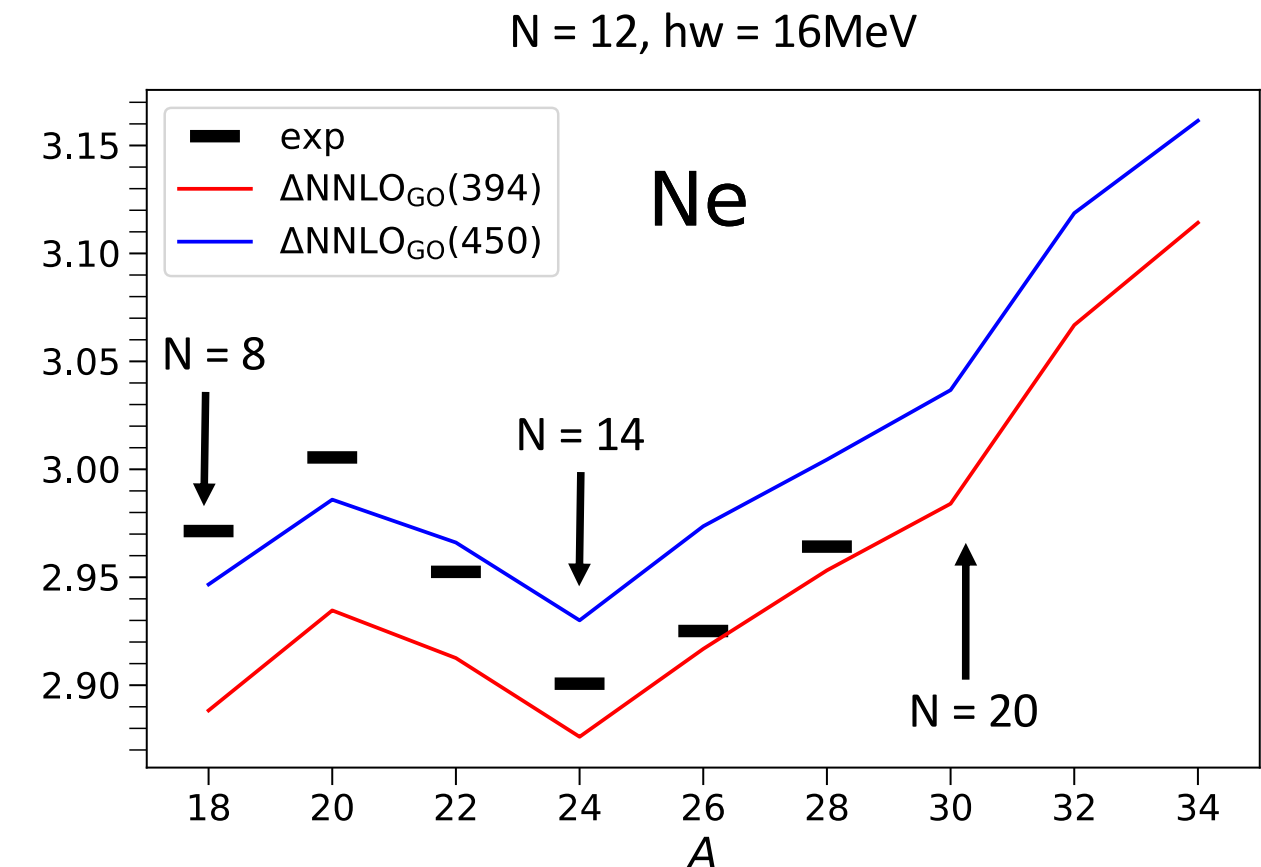
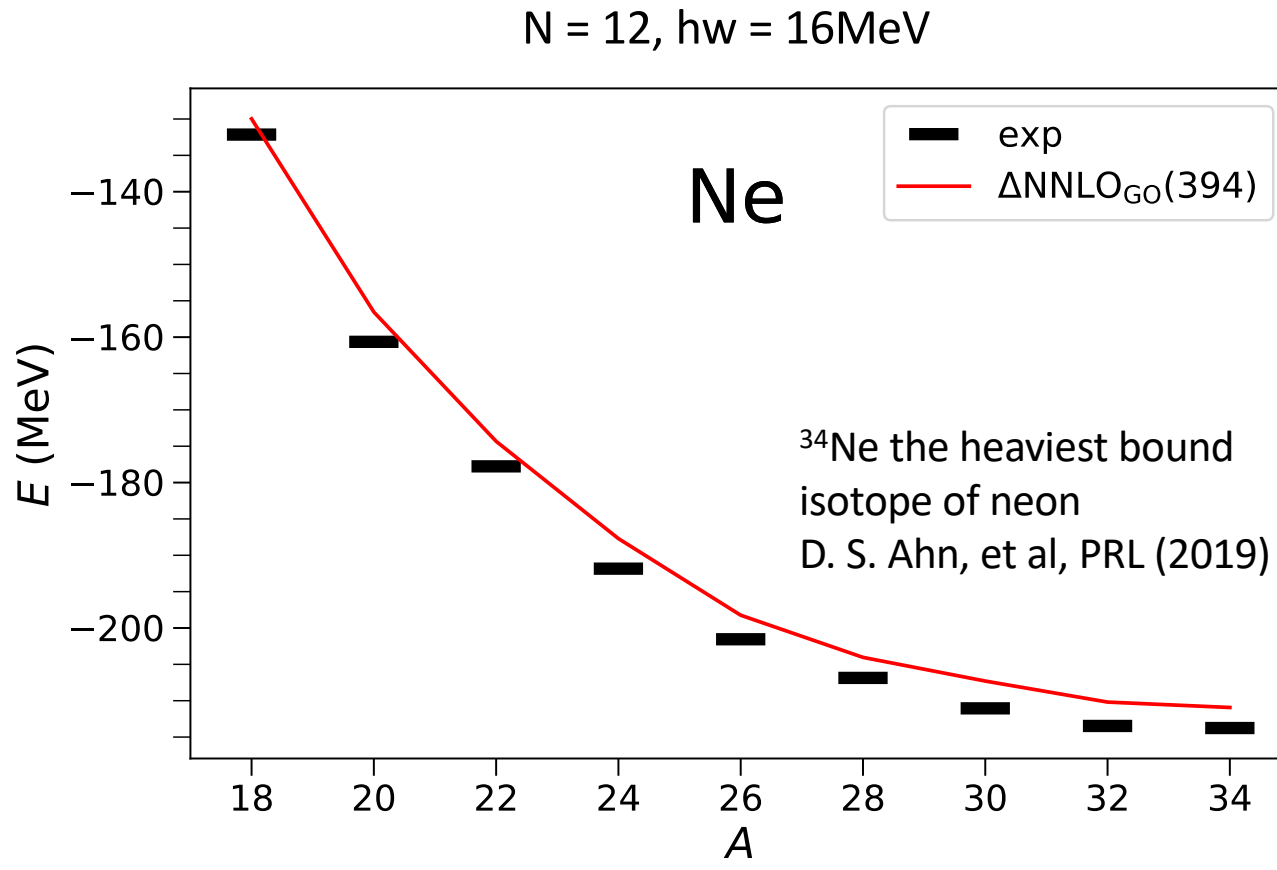
Coupled-cluster computations of deformed nuclei – natural orbitals



- Coupled-cluster calculations from axially symmetric reference states
- Natural orbitals from many-body perturbation theory [A. Tichai, et al PRC (2019)] yields rapid convergence with respect 3p3h excitations in CCSDT-1
- Hartree-Fock with projection after variation (PAV) gives upper bound on the energy gain from symmetry restoration

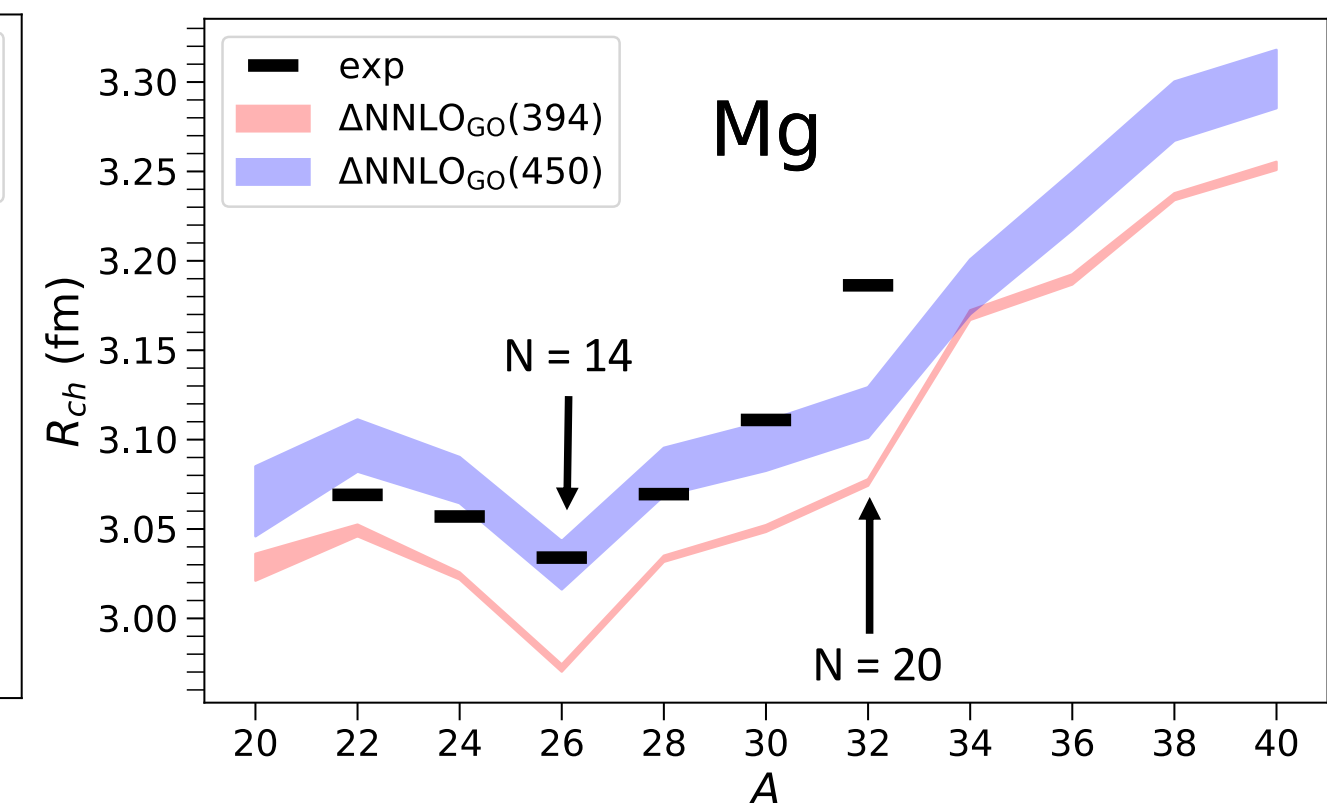
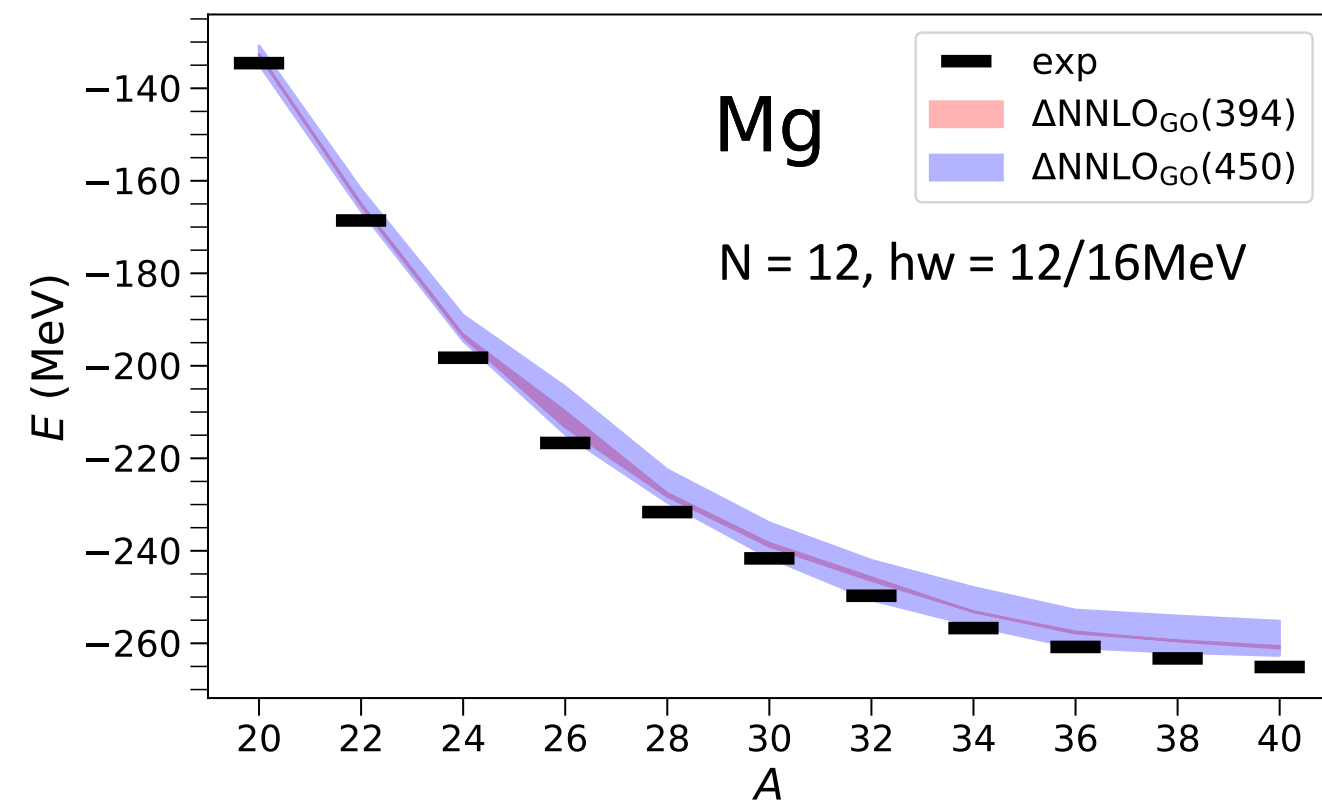
Computations of neon isotopes

- Dripline correctly predicted at ^{34}Ne
- Charge radii predicts shell closures at $N = 8$, $N = 14$, and at $N = 20$



Computations of magnesium isotopes

- Dripline predicted at ^{40}Mg – continuum may impact the location of the dripline
- Charge radii predicts shell closures at $N = 8$, $N = 14$, and at $N = 20$
- The bands indicate uncertainties from model-space truncations



Symmetry restored coupled-cluster theory

Projection after variation (PAV):

$$E_J = \frac{\langle \tilde{\Psi} | P_J H | \Psi \rangle}{\langle \tilde{\Psi} | P_J | \Psi \rangle}$$

Right state is parametrized: $|\Psi\rangle = e^T |\Phi_0\rangle$

Left state is parametrized as:

$$\langle \tilde{\Psi} | = \langle \Phi_0 | (1 + \Lambda) e^{-T} \quad \text{or} \quad \langle \tilde{\Psi} | = \langle \Phi_0 |$$



Coupled-cluster bi-variational energy expression



Naïve energy expression

The total energy of a nucleus



$$E = E_{\text{ref}} + \Delta E_{\text{CCSD}} + \Delta E_{\text{CCSdT-1}} + \delta E$$



Image credit: Wikimedia Commons

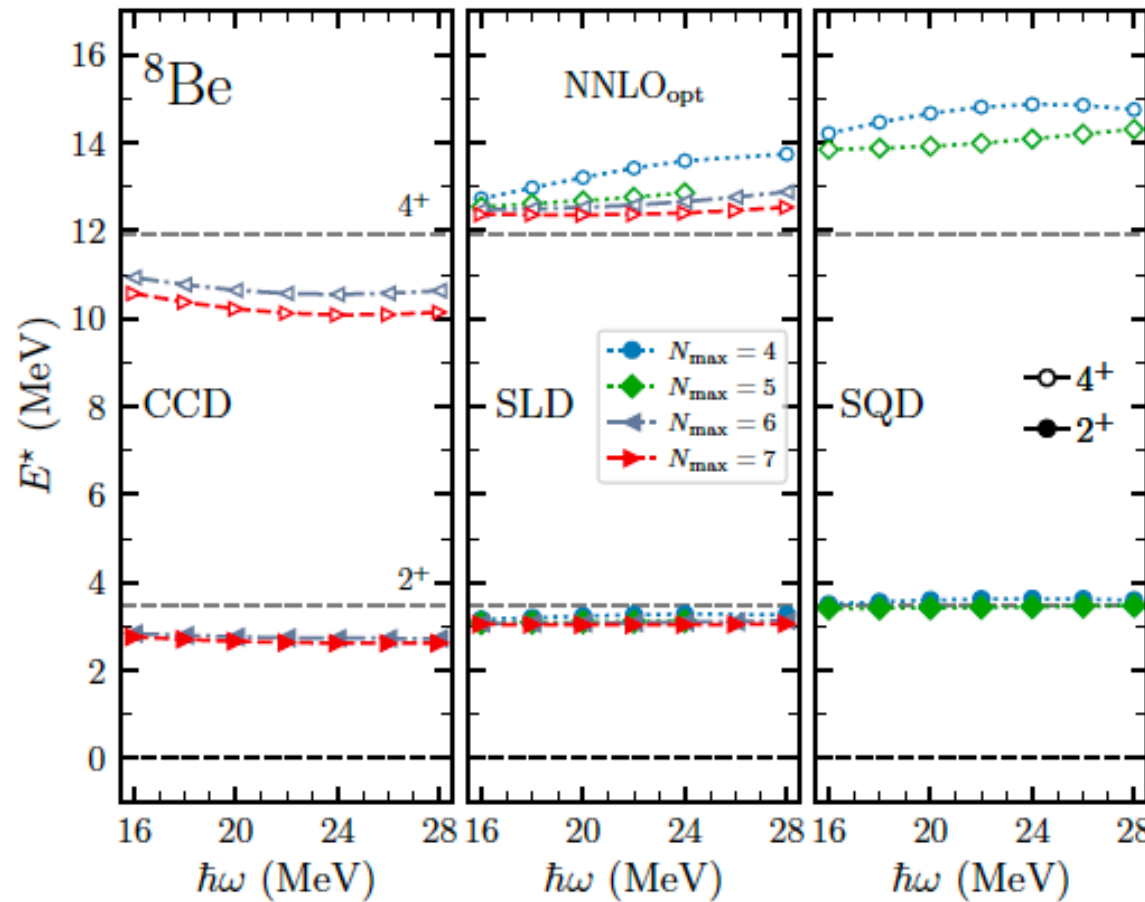
Dynamic correlation (large contribution and requires size-extensive methods)

Static correlation (can use non size-extensive methods)

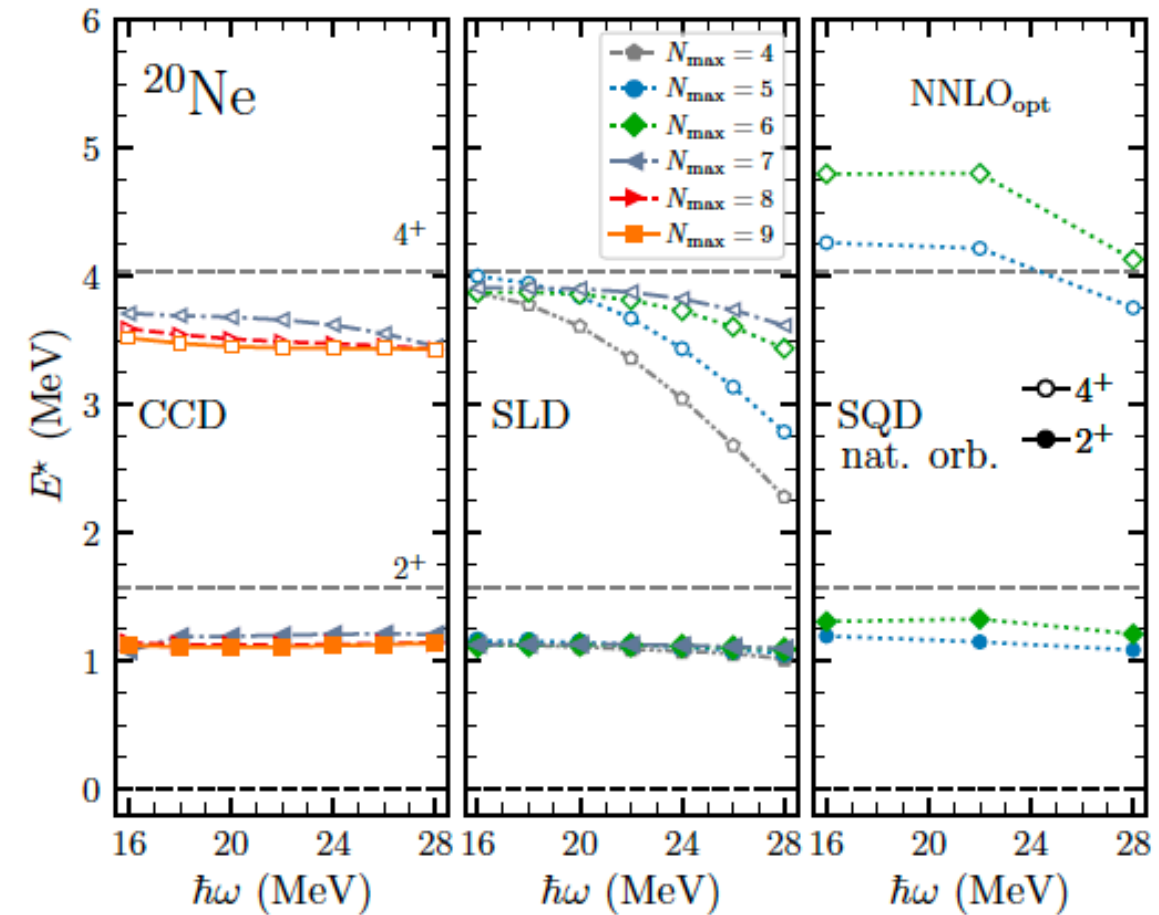
Benchmark computation for ^8Be and ^{20}Ne

G. Hagen et al, arXiv:2201.07298 (2022)

Benchmarks from NCSM
[Caprio, Maris, Vary & Smith (2015)]



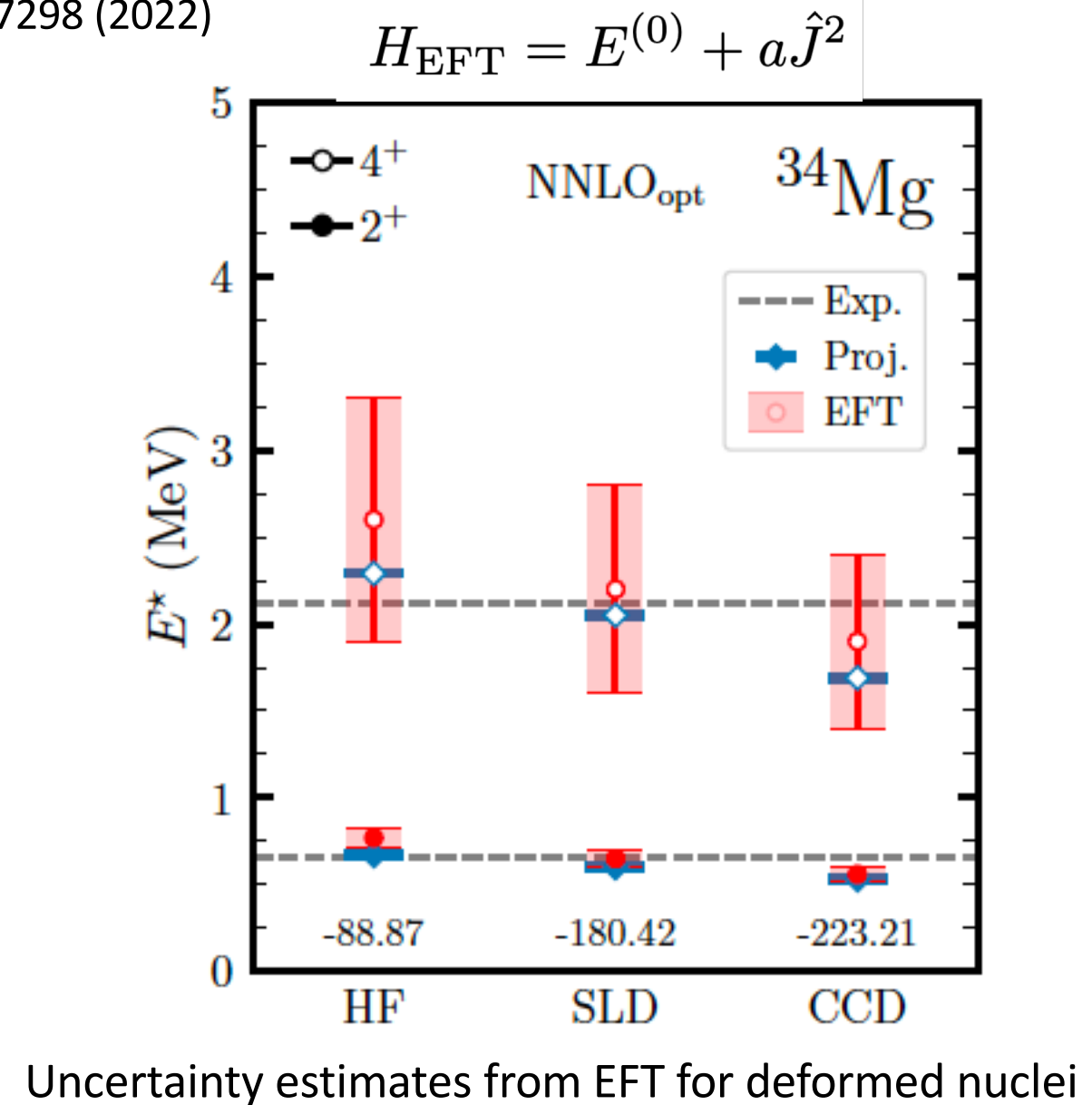
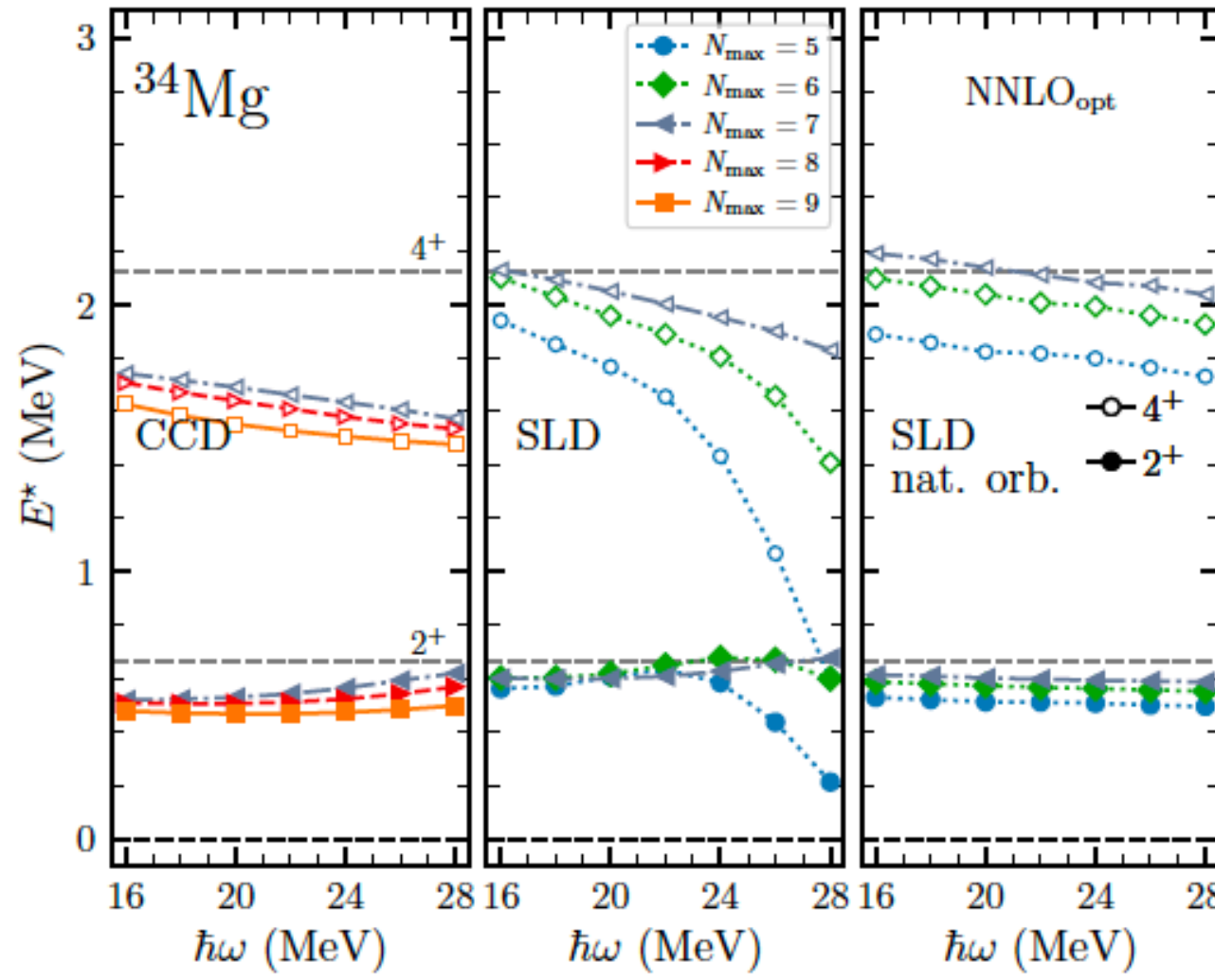
Benchmarks from Symmetry-Adapted NCSM
[Dytrych, Launey et al. (2020)]



CCD spectra a bit too compressed, but we are getting there ...

Computation of ^{34}Mg

G. Hagen et al, arXiv:2201.07298 (2022)



Summary of results

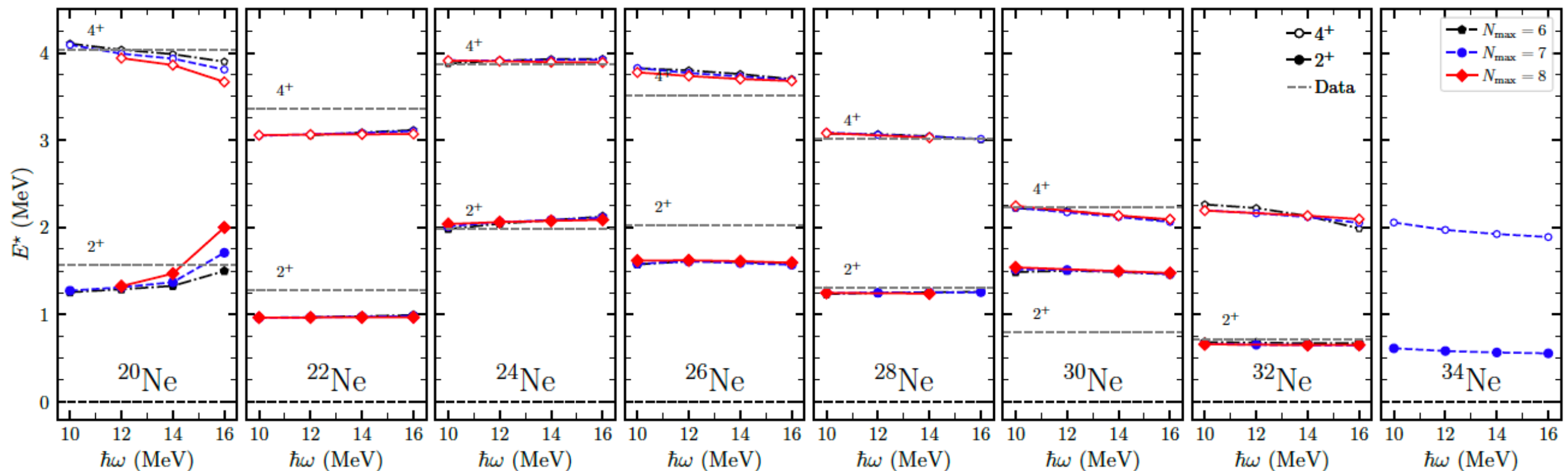
- Symmetry projection has little impact on radii
- Matched low-energy constants to the rigid rotor model (leading order EFT for rotations)
- The EFT accurately reproduces rotational bands

	Unprojected			Projected					EFT	
	E	$\langle J^2 \rangle$	R_{ch} (fm)	δE	$E^{(0)} = E + \delta E$	R_{ch} (fm)	$E^{(2)} - E^{(0)}$	$E^{(4)} - E^{(0)}$	$E^{(2)} - E^{(0)}$	$E^{(4)} - E^{(0)}$
^{20}Ne										
HF	-59.442	22.778	2.623	-5.760	-65.202	2.619	1.26	4.34	1.5 ± 0.1	5.1 ± 1.3
SLD	-122.467	19.059	2.601	-4.332	-126.799	2.598	1.13	3.90	1.4 ± 0.1	4.5 ± 1.2
CCD	-142.666	16.128	2.621	-3.627	-146.293	2.620	1.19	3.68	1.3 ± 0.1	4.5 ± 1.2

	Unprojected			Projected					EFT	
	E	$\langle J^2 \rangle$	R_{ch} (fm)	δE	$E^{(0)} = E + \delta E$	R_{ch} (fm)	$E^{(2)} - E^{(0)}$	$E^{(4)} - E^{(0)}$	$E^{(2)} - E^{(0)}$	$E^{(4)} - E^{(0)}$
^{34}Mg										
HF	-85.687	24.740	2.727	-3.184	-88.87	2.724	0.67	2.29	0.77 ± 0.06	2.6 ± 0.7
SLD	-177.938	22.790	2.707	-2.479	-180.42	2.704	0.60	2.05	0.65 ± 0.05	2.2 ± 0.6
CCD	-221.315	20.213	2.725	-1.893	-223.21	2.722	0.53	1.69	0.56 ± 0.04	1.9 ± 0.5

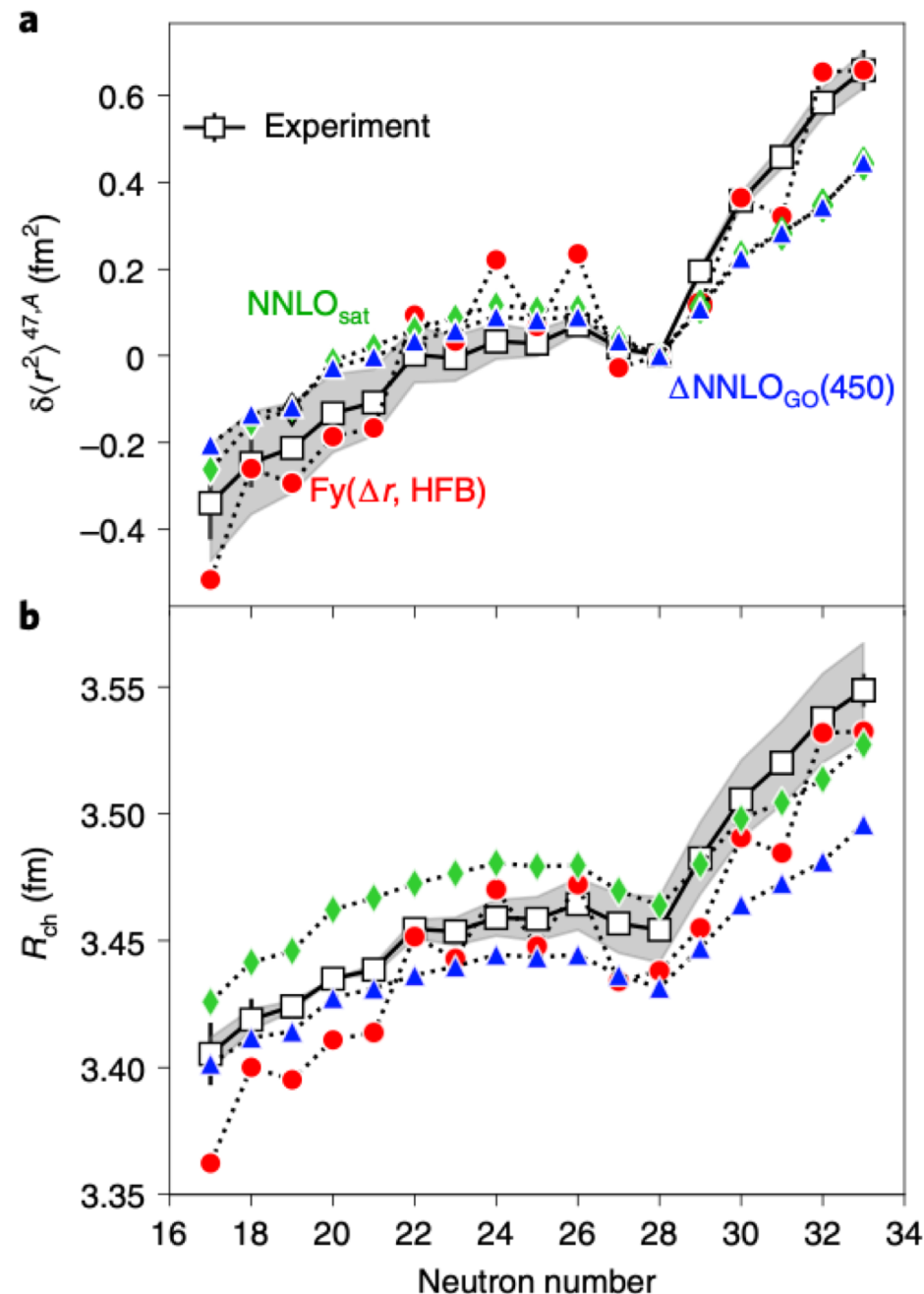
Neon isotopes: Inclusion of three-body forces and more accurate left state

Rotational structure of neutron-rich neon isotopes in good agreement with data



Interaction 1.8/2.0(EM) from Hebeler et al (2012) over-emphasizes $N=20$ shell closure
 $^{32,34}\text{Ne}$ are as rotational as ^{34}Mg

Charge radii of neutron-rich potassium isotopes

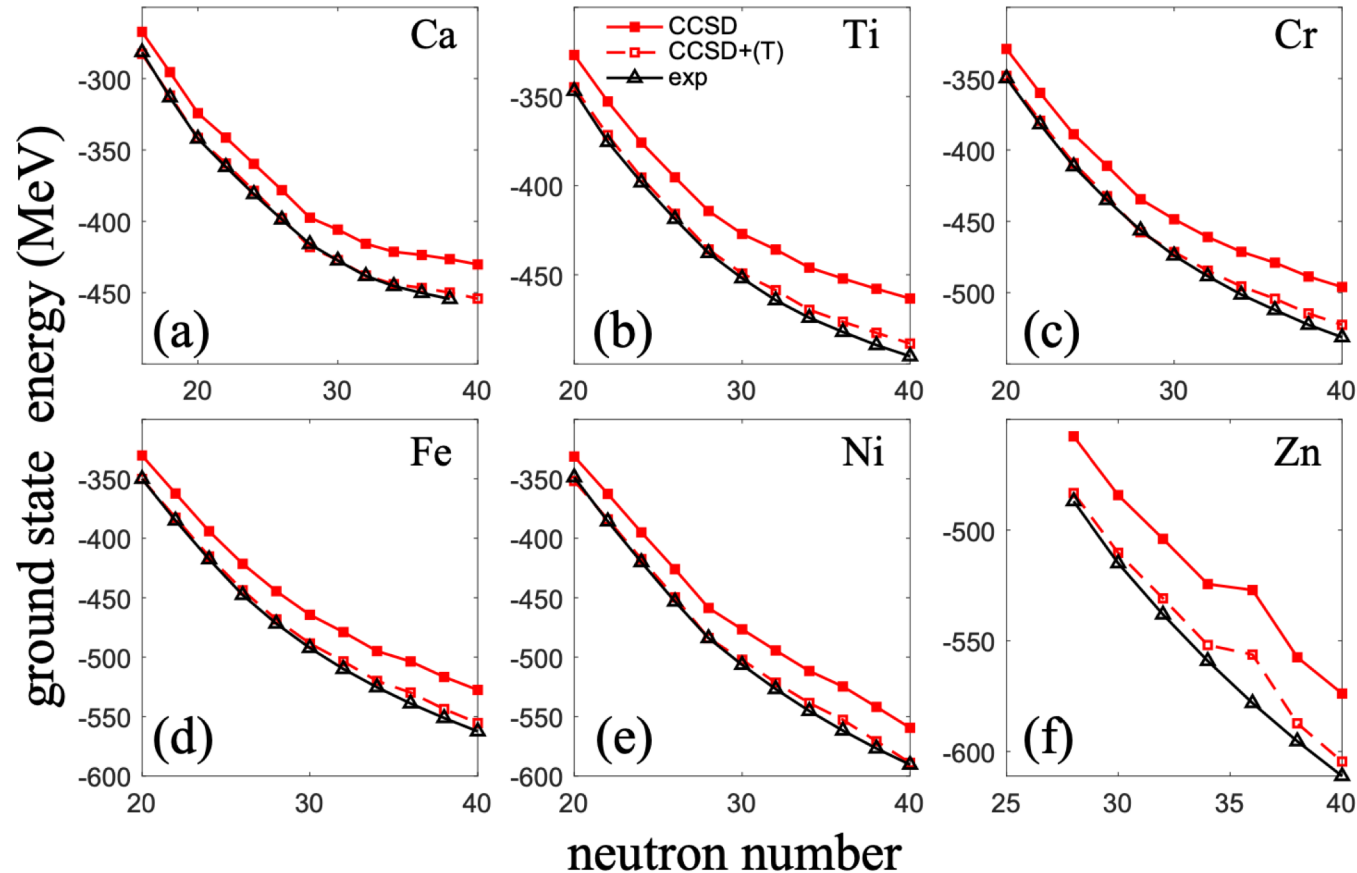


- First high precision measurement of ^{52}K charge radius by CRIS @ ISOLDE/CERN
- Steep increase in charge radii beyond $N = 28$ challenges theory
- No signature of $N = 32$ shell closure
- Isotope shifts not sensitive to details of NNLO chiral Hamiltonians

Coupled-cluster computations of even-even Ca-Zn nuclei

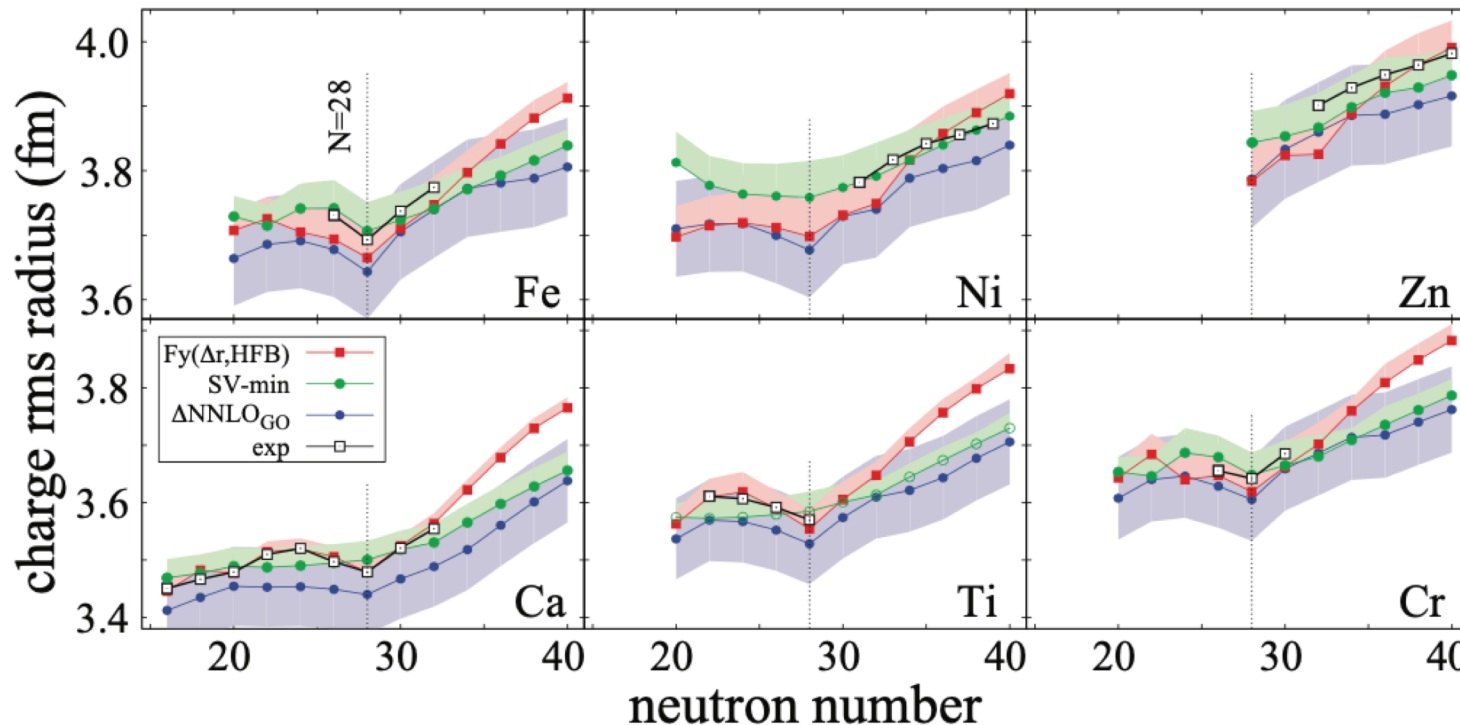
- We construct natural orbitals from a Hartree-Fock calculation using $N_{\text{max}} = 14$.
- The normal-ordered Hamiltonian in natural orbitals is truncated to a smaller model-space (See J. Hoppe et al. Phys. Rev. C 103, 014321 (2021))
- We achieve rapid convergence for energies and radii

$N_{\text{max}}^{\text{nat}}$	$\hbar\omega=12 \text{ MeV}$		$\hbar\omega=16 \text{ MeV}$	
	$E(\text{MeV})$	$R_{\text{ch}}(\text{fm})$	$E(\text{MeV})$	$R_{\text{ch}}(\text{fm})$
6	-473.731	3.857	-474.445	3.848
8	-513.502	3.882	-515.685	3.869
10	-520.787	3.896	-523.355	3.882
12	-521.746	3.900	-524.384	3.886



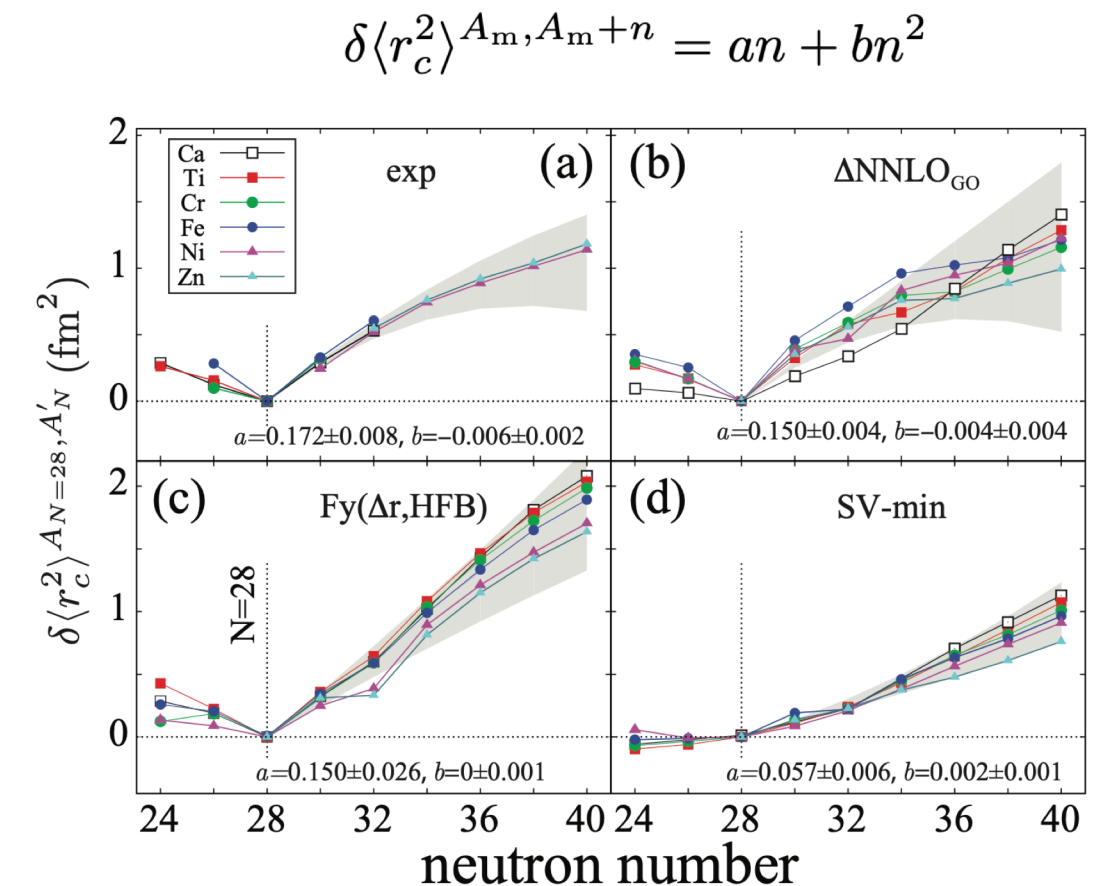
CCSD ground-state energies with estimated triples
(12% of CCSD correlation energy)

Coupled-cluster computations of even-even Ca-Zn nuclei

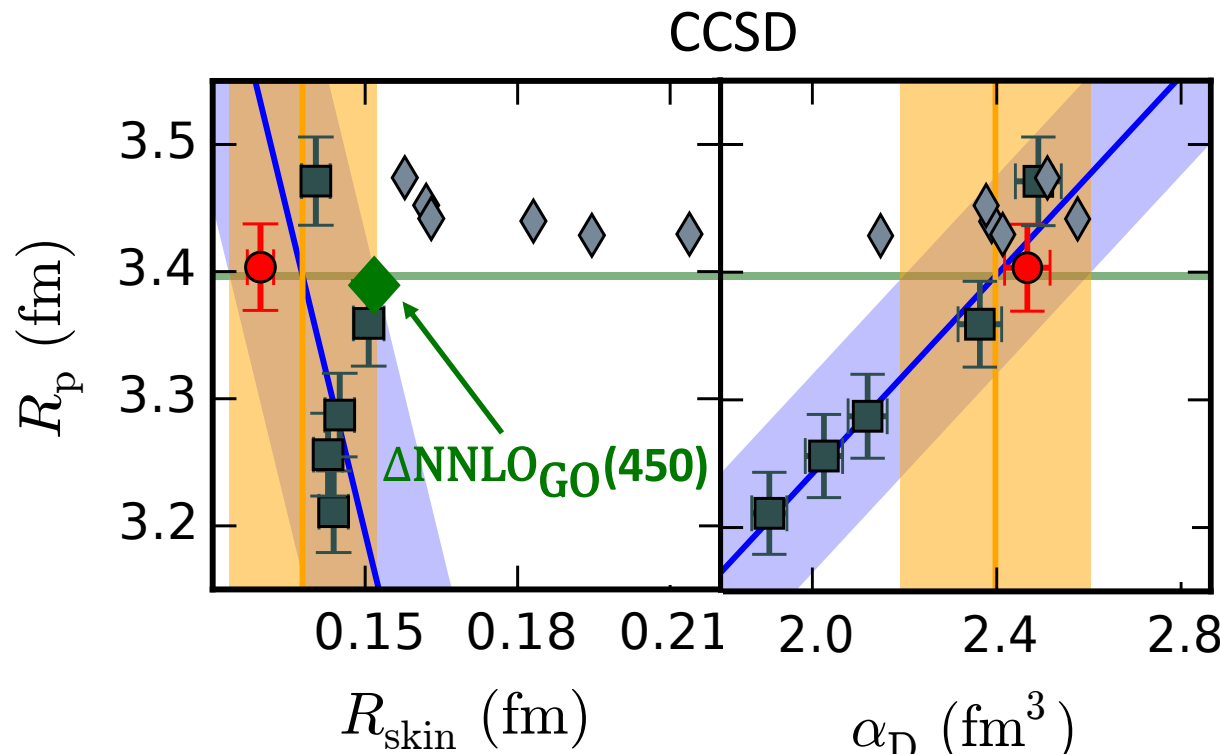


M. Kortelainen, Z. H. Sun, G. Hagen, W. Nazarewicz, T. Papenbrock,
P-G. Reinhard, Phys. Rev. C 105, L021303 (2022)

Element independent increase in radii beyond $N = 28$ for Ca-Zn isotopes
The trend is explained by fitting the Z averaged isotope shift to a parabolic expression from generalized seniority picture



Neutron skin and dipole polarizability of ^{48}Ca

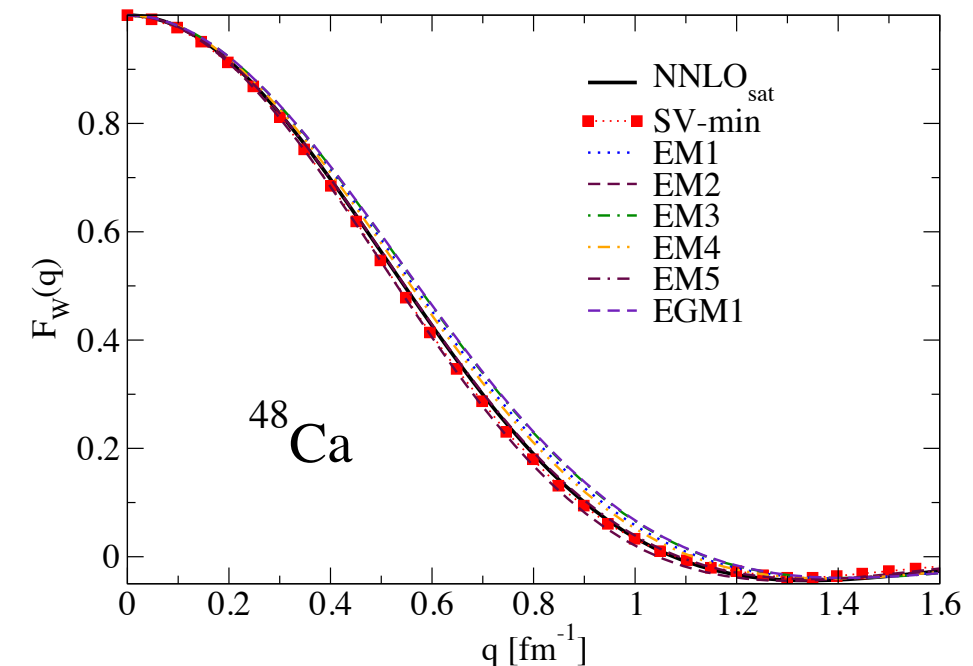
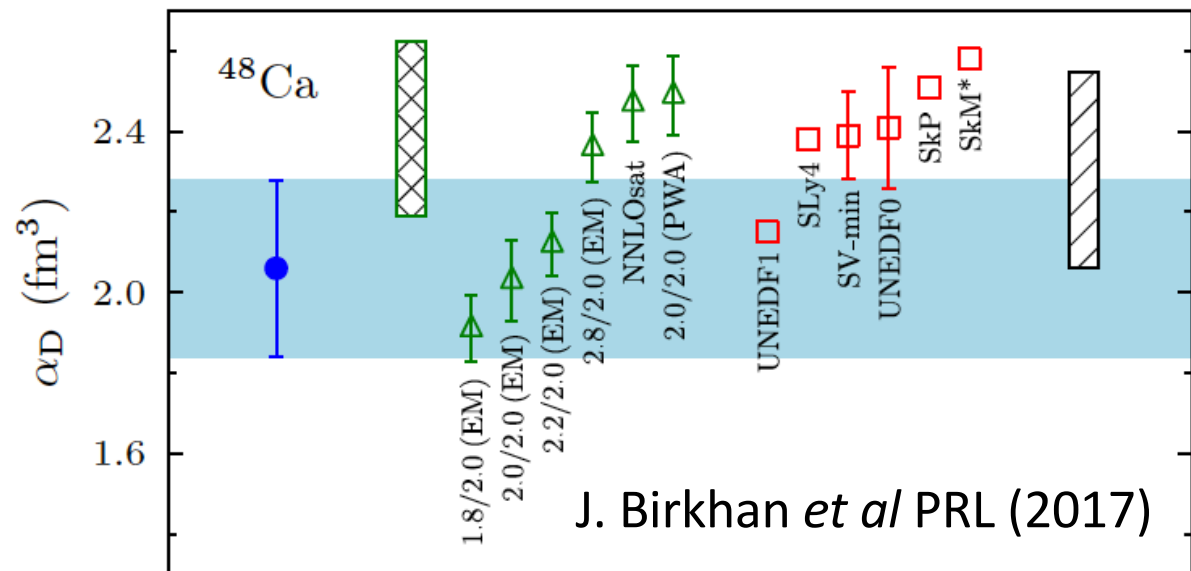


G. Hagen *et al*, Nature Physics **12**, 186–190 (2016)

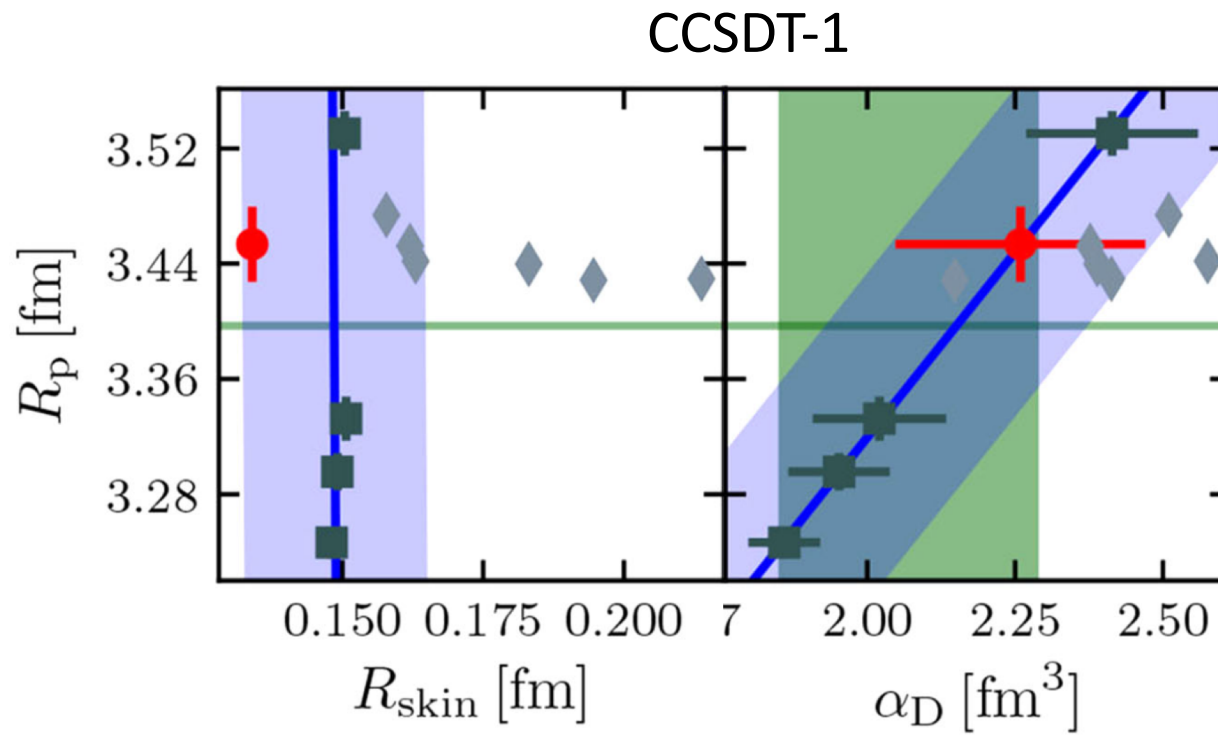
- Neutron skin significantly smaller than in DFT
 - Results for ^{48}Ca agrees with CREX
- $R_{\text{skin}} = 0.121 \pm 0.035\text{fm}$

CREX: $F_w(q = 0.873 \text{ fm}^{-1}) = 0.1304 \pm 0.0052$

Coupled-Cluster: $0.102 \leq F_w(q = 0.873 \text{ fm}^{-1}) \leq 0.161$



Neutron skin and dipole polarizability of ^{48}Ca

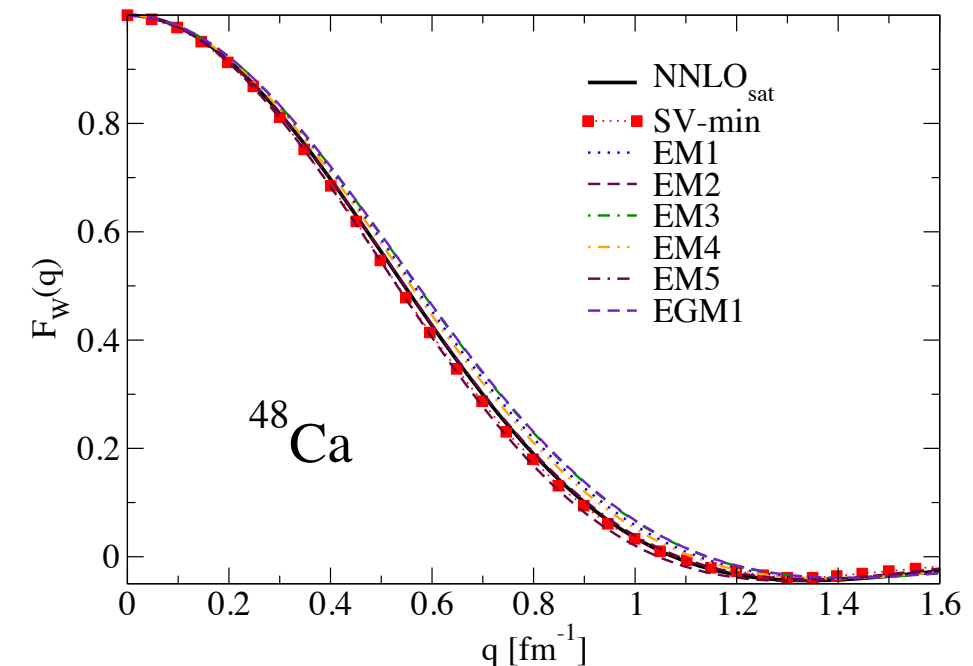
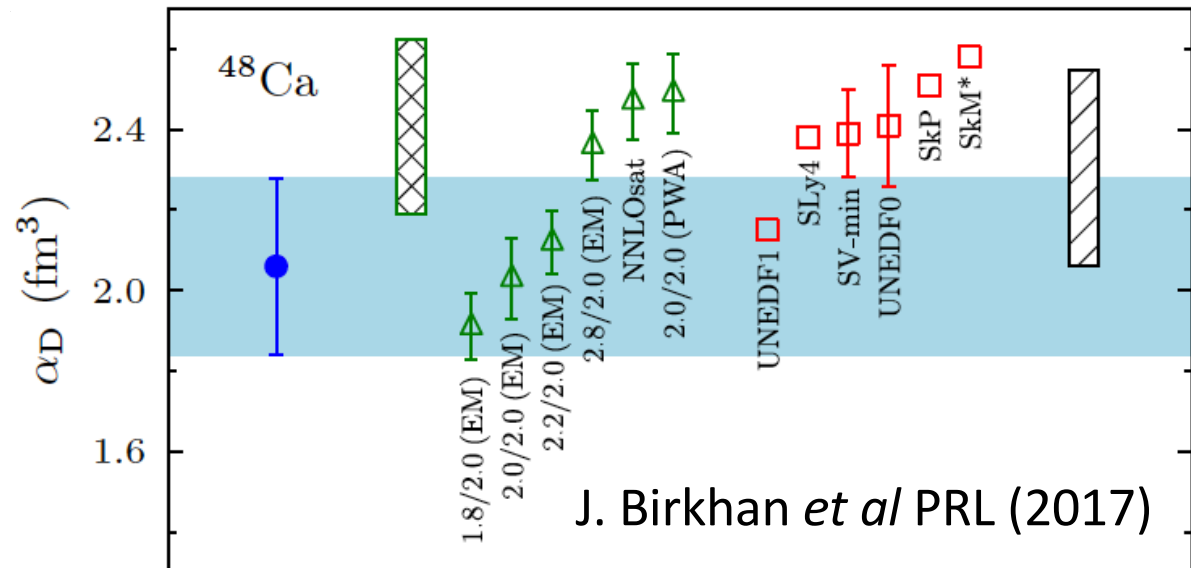


J. Simonis, S. Bacca1, and G. Hagen Eur. Phys. J. A 55 (2019)

- Neutron skin significantly smaller than in DFT
 - Results for ^{48}Ca agrees with CREX
- $R_{\text{skin}} = 0.121 \pm 0.035\text{fm}$

CREX: $F_w(q = 0.873 \text{ fm}^{-1}) = 0.1304 \pm 0.0052$

Coupled-Cluster: $0.102 \leq F_w(q = 0.873 \text{ fm}^{-1}) \leq 0.161$

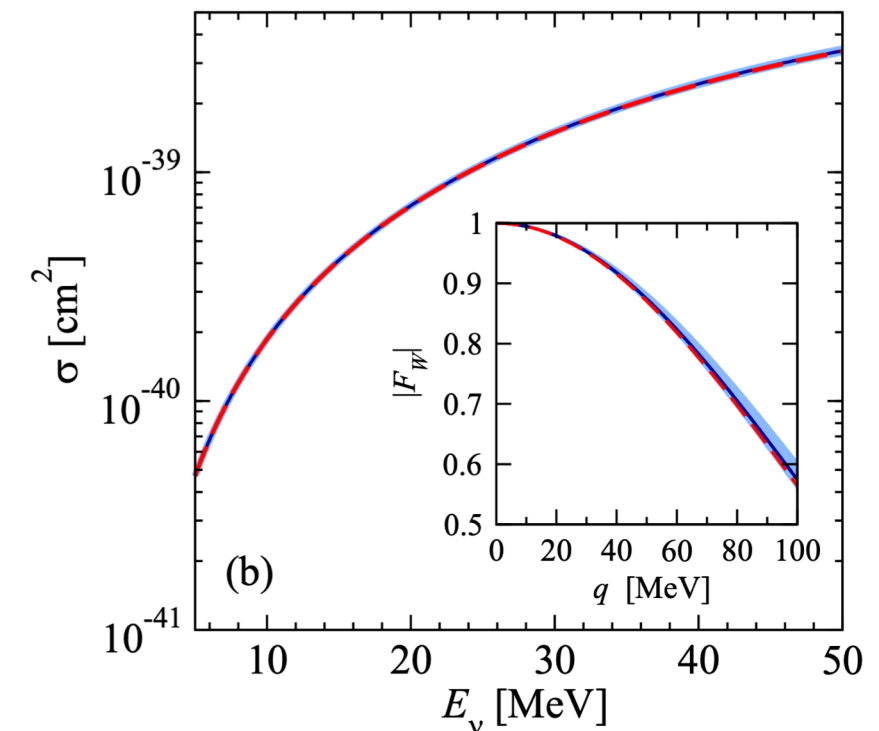
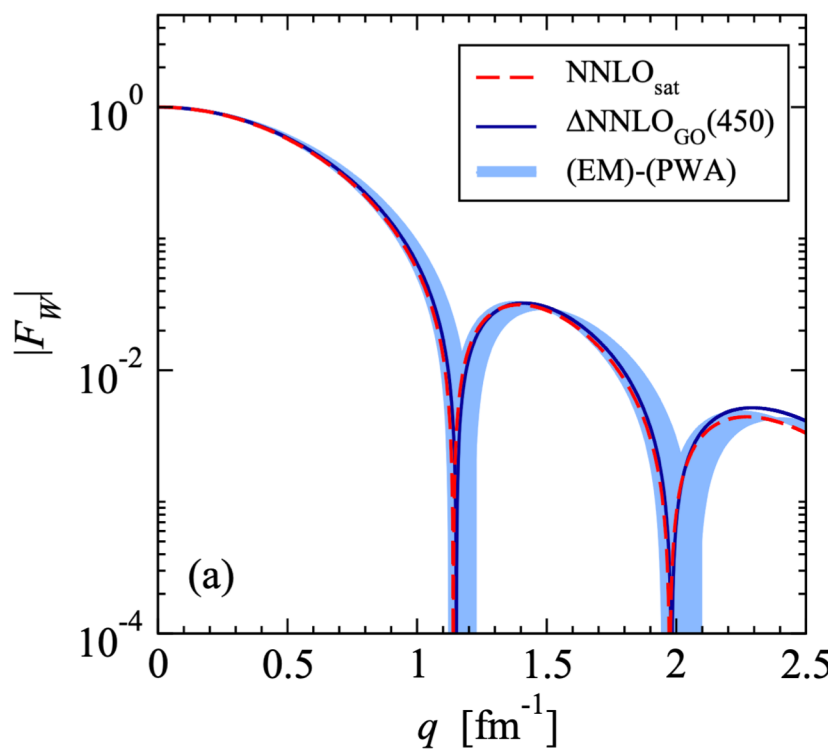
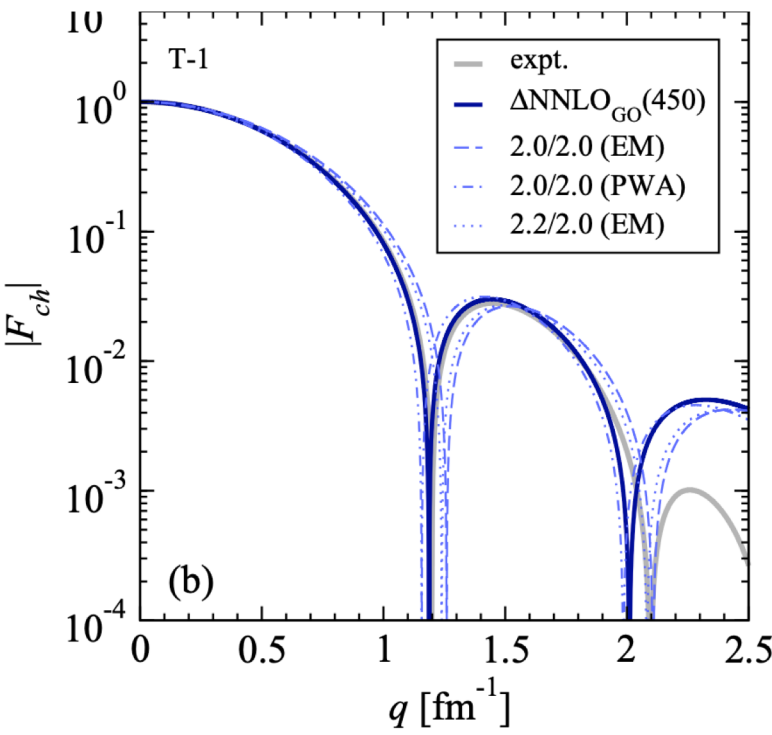


Coherent elastic neutrino scattering (CE ν NS) on ^{40}Ar

Coherent cross section

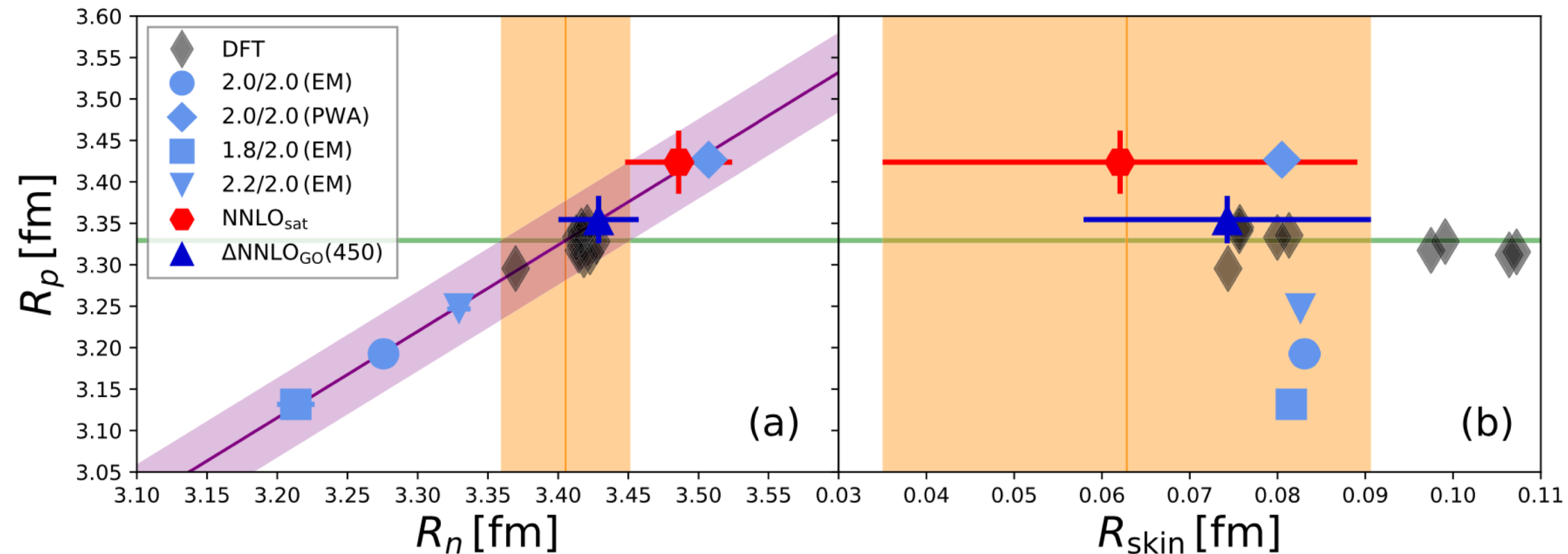
$$\frac{d\sigma}{dT}(E_\nu, T) \simeq \frac{G_F^2}{4\pi} M \left[1 - \frac{MT}{2E_\nu^2} \right] Q_W^2 F_W^2(q^2)$$

- Good agreement with data for charge form-factor in ^{40}Ar
- Mild sensitivity to employed interaction in energy region relevant to coherent scattering
- Need higher-precision experiments in order to inform/constrain nuclear models

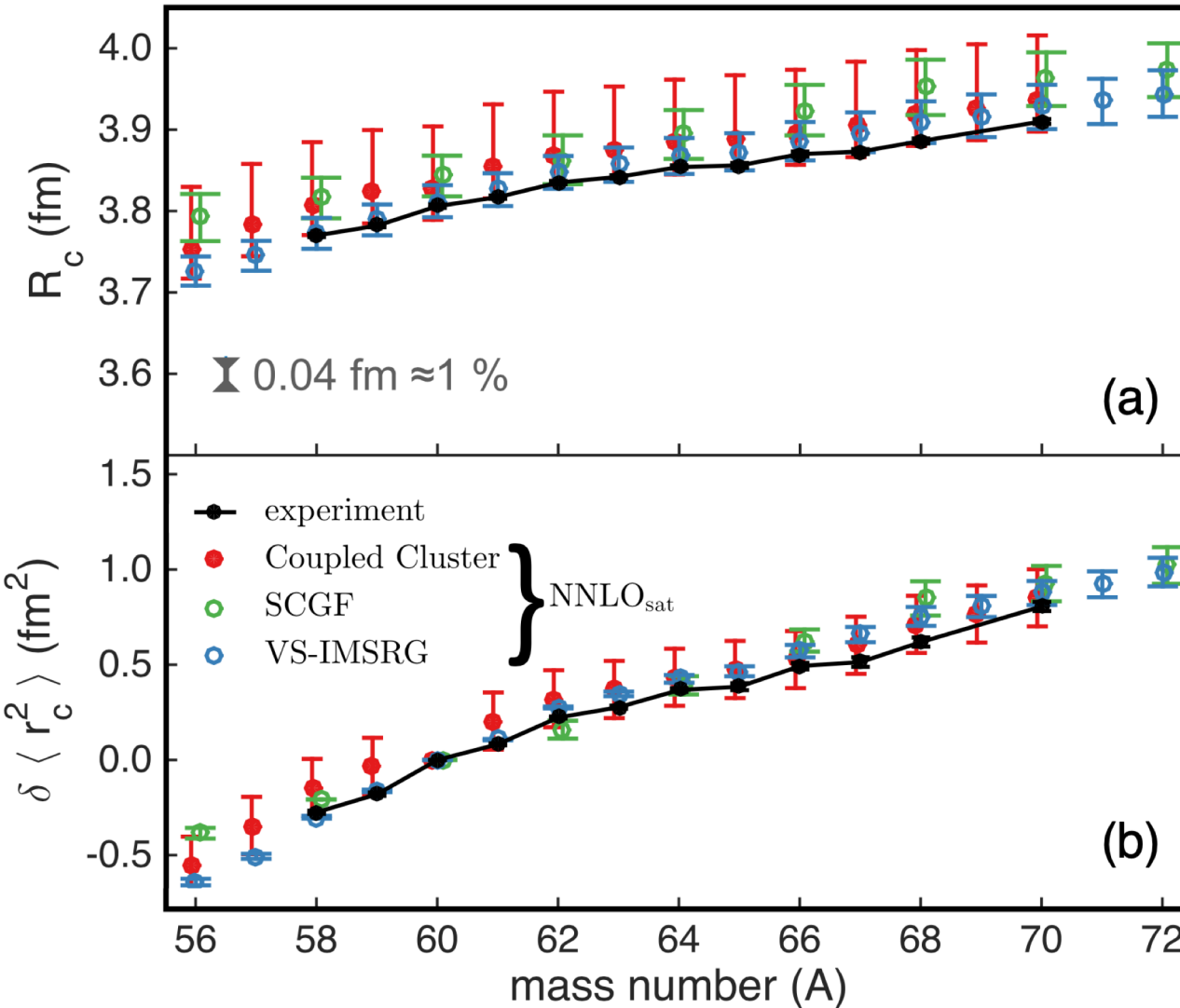


Coherent elastic neutrino scattering (CE ν NS) on ^{40}Ar

The neutron radius and skin of ^{40}Ar from coupled cluster with interactions from chiral EFTs are consistent with DFT predictions – This is contrary to the case of ^{48}Ca



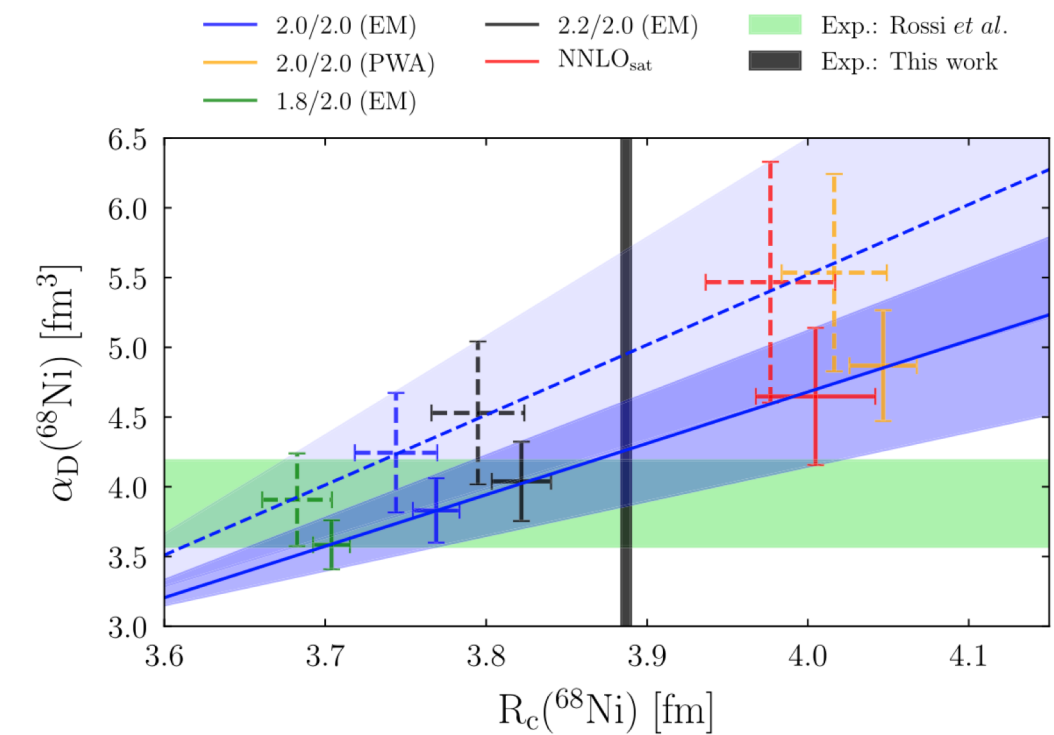
Radii, skins, and dipole polarizability of nickel isotopes



S. Malbrunot-Ettenauer, et al, Phys. Rev. Lett. 128, 022502 (2022)

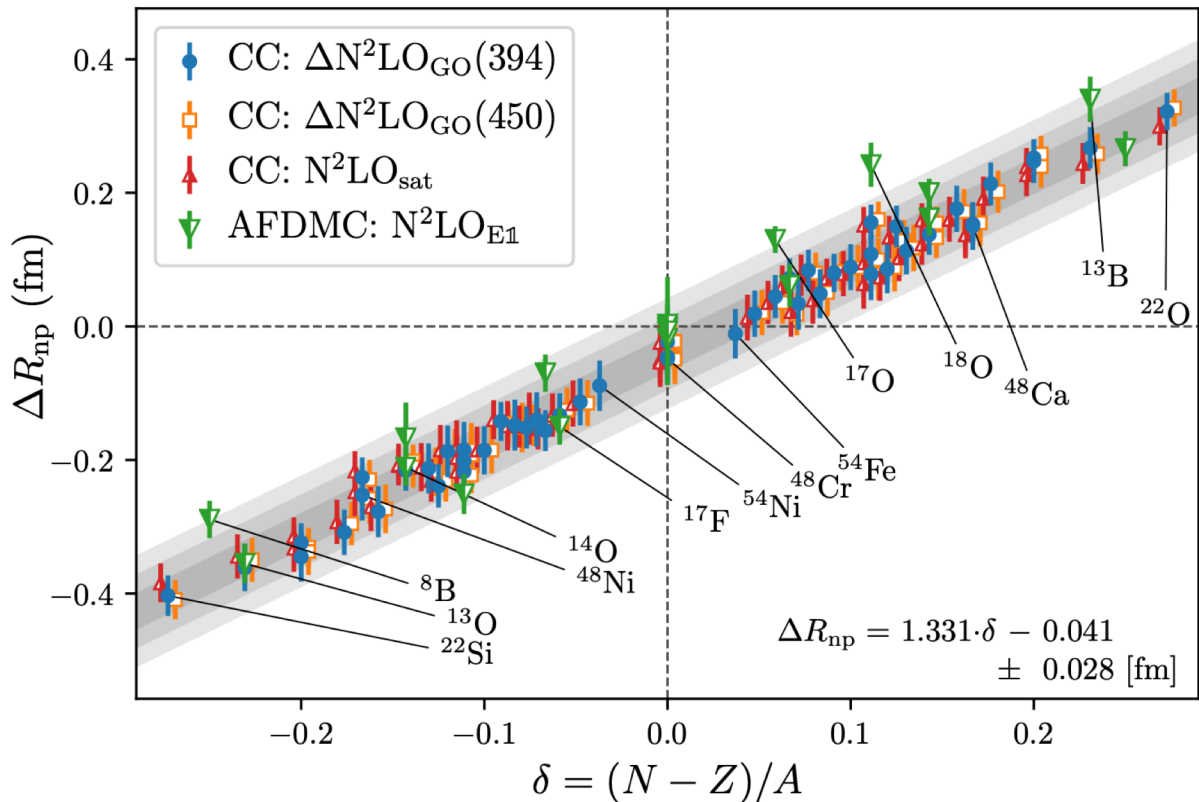
Kaufmann et al, Phys. Rev. Lett. 124, 132502 (2020)

Hamiltonian	α_D	R_p	R_n	R_{skin}	R_c
1.8/2.0 (EM)	3.58(18)	3.62(1)	3.82(1)	0.201(1)	3.70(1)
2.0/2.0 (EM)	3.83(23)	3.69(2)	3.89(2)	0.202(3)	3.77(1)
2.2/2.0 (EM)	4.04(28)	3.74(2)	3.94(2)	0.203(4)	3.82(2)
2.0/2.0 (PWA)	4.87(40)	3.97(2)	4.17(3)	0.204(8)	4.05(2)
NNLO _{sat}	4.65(49)	3.93(4)	4.11(5)	0.183(8)	4.00(4)



Trends of neutron skins of mirror nuclei

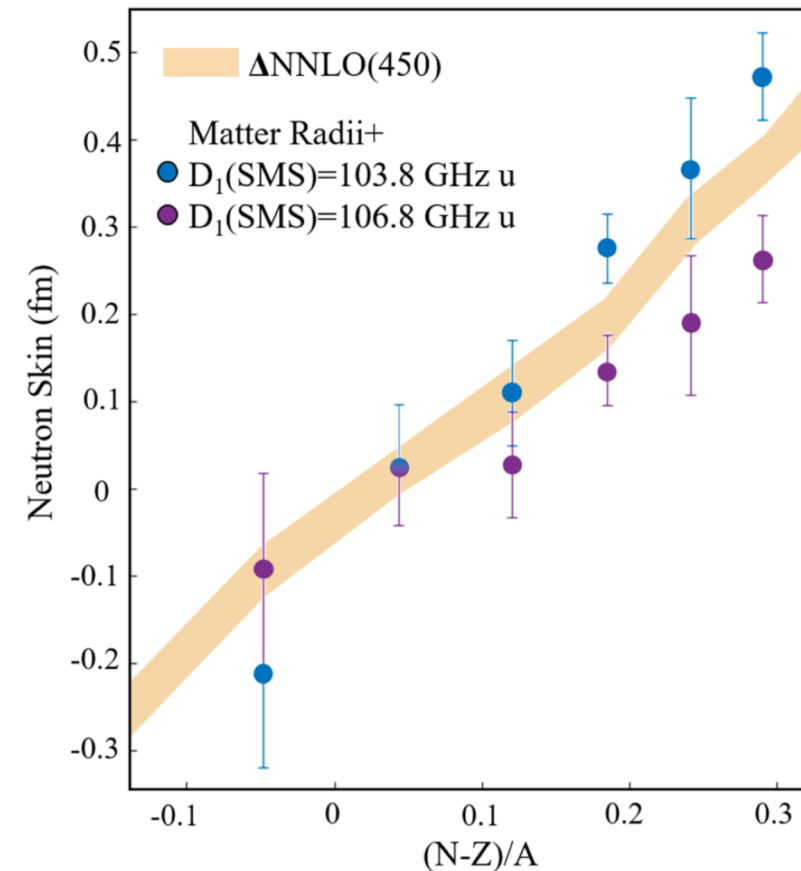
S. J. Novario, D. Lonardoni, S. Gandolfi, G. Hagen,
arXiv:2111.12775 (2022)



Different methods and interactions give a linear relation between neutron skin and isospin asymmetry

$$\delta(^{208}\text{Pb}) = 44/208 = 0.212$$

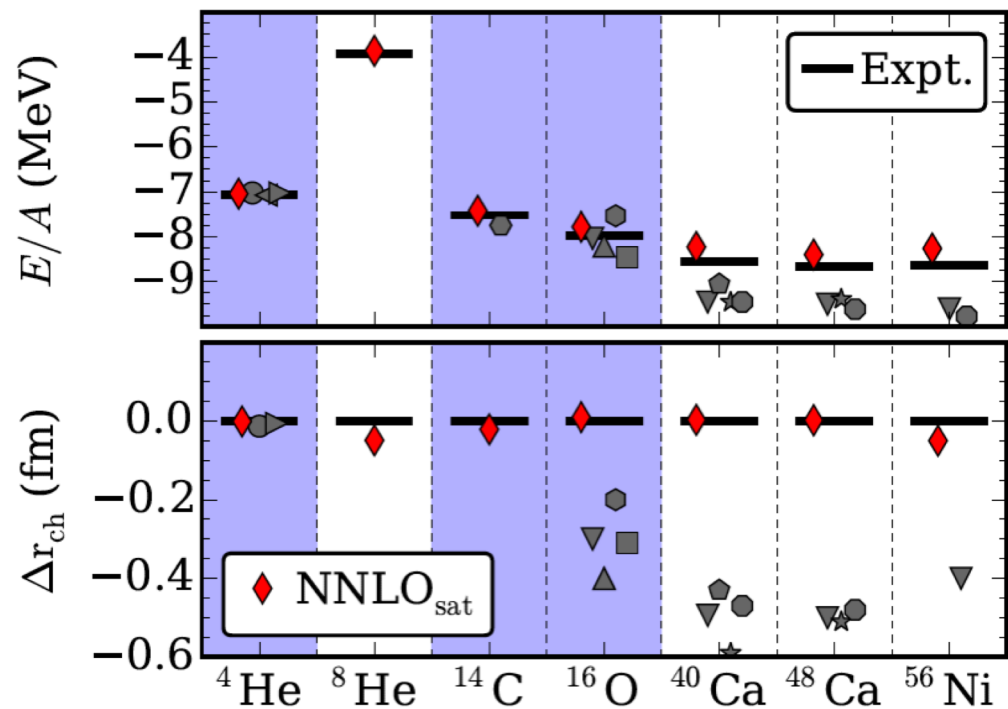
$$\Delta R_{np}(^{208}\text{Pb}) = 0.241 \pm 0.028 \text{ fm}$$



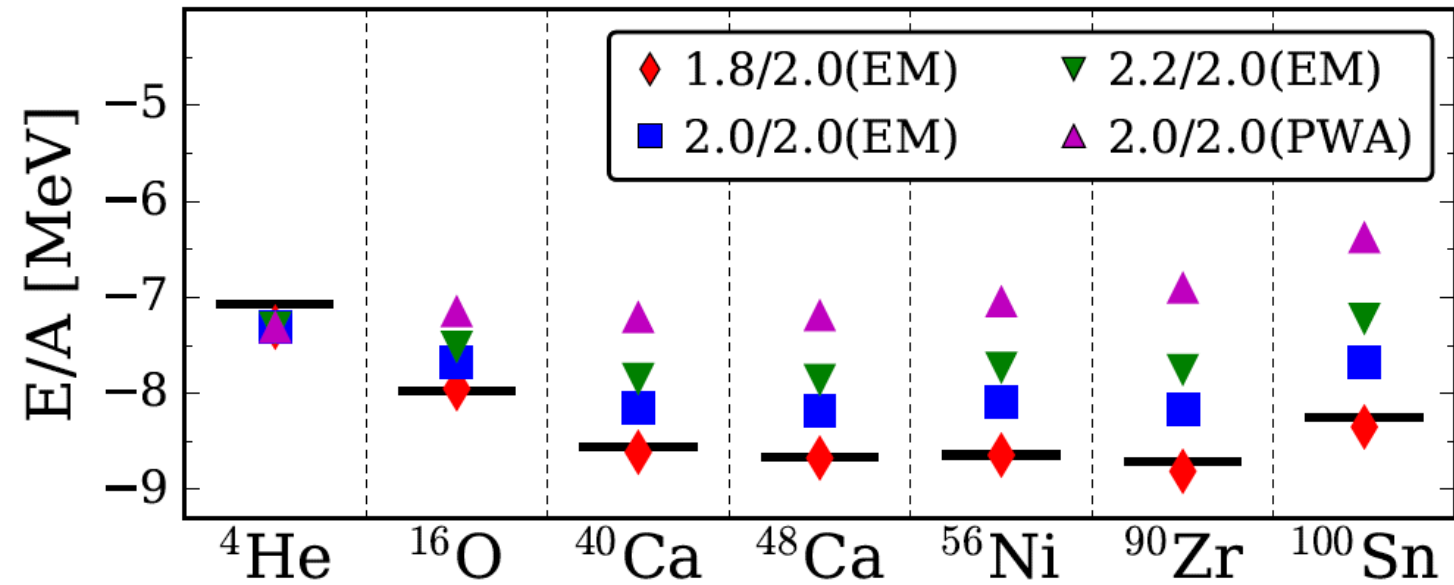
Neutron skin of sodium isotopes as a function of isospin asymmetry. Data used available matter radii and charge radii from isotope shift measurements using two different values of the atomic parameter K_{SMS}

B. Ohayon, R. F. Garcia Ruiz, Z. H. Sun, G. Hagen, T. Papenbrock, B. K. Sahoo, Phys. Rev. C **105**, L031305 (2022)

Why do some interaction models work better than others?



A. Ekström *et al*, Phys. Rev. C **91**, 051301(R) (2015).



K. Hebeler *et al* PRC (2011).
T. Morris *et al*, PRL (2018).

To answer this we need predictions with rigorous **uncertainty quantification** and **sensitivity analyses** that are grounded in the description of the underlying nuclear Hamiltonian

Andreas Ekström, Gaute Hagen PRL **123**, 252501 (2019)

Global sensitivity analysis of the radius and binding energy of 16-O

Sensitivity analysis addresses the question ‘How much does each model parameter contribute to the uncertainty in the prediction?’

Global methods deal with the uncertainties of the outputs due to input variations over the whole domain.

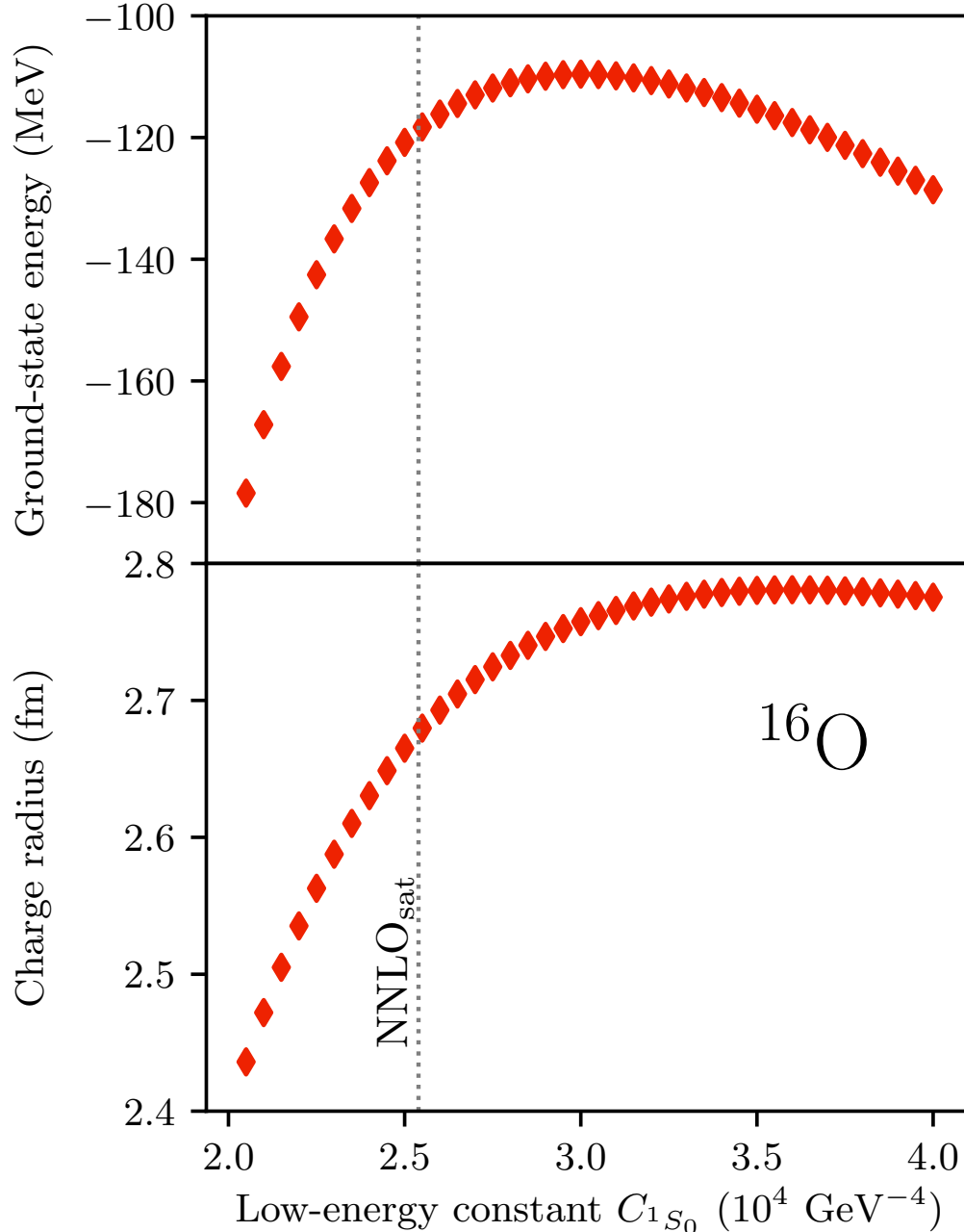
Computational bottleneck

A global sensitivity analyses of the binding energy and charge radius of a nucleus like 16-O requires more than one million model evaluations



Sub-space projected coupled-cluster

Andreas Ekström, Gaute Hagen PRL **123**, 252501 (2019)



- Generalization of the eigenvector continuation method [Frame D. et al., Phys. Rev. Lett. **121**, 032501 (2018)]
- Write the Hamiltonian in a linearized form

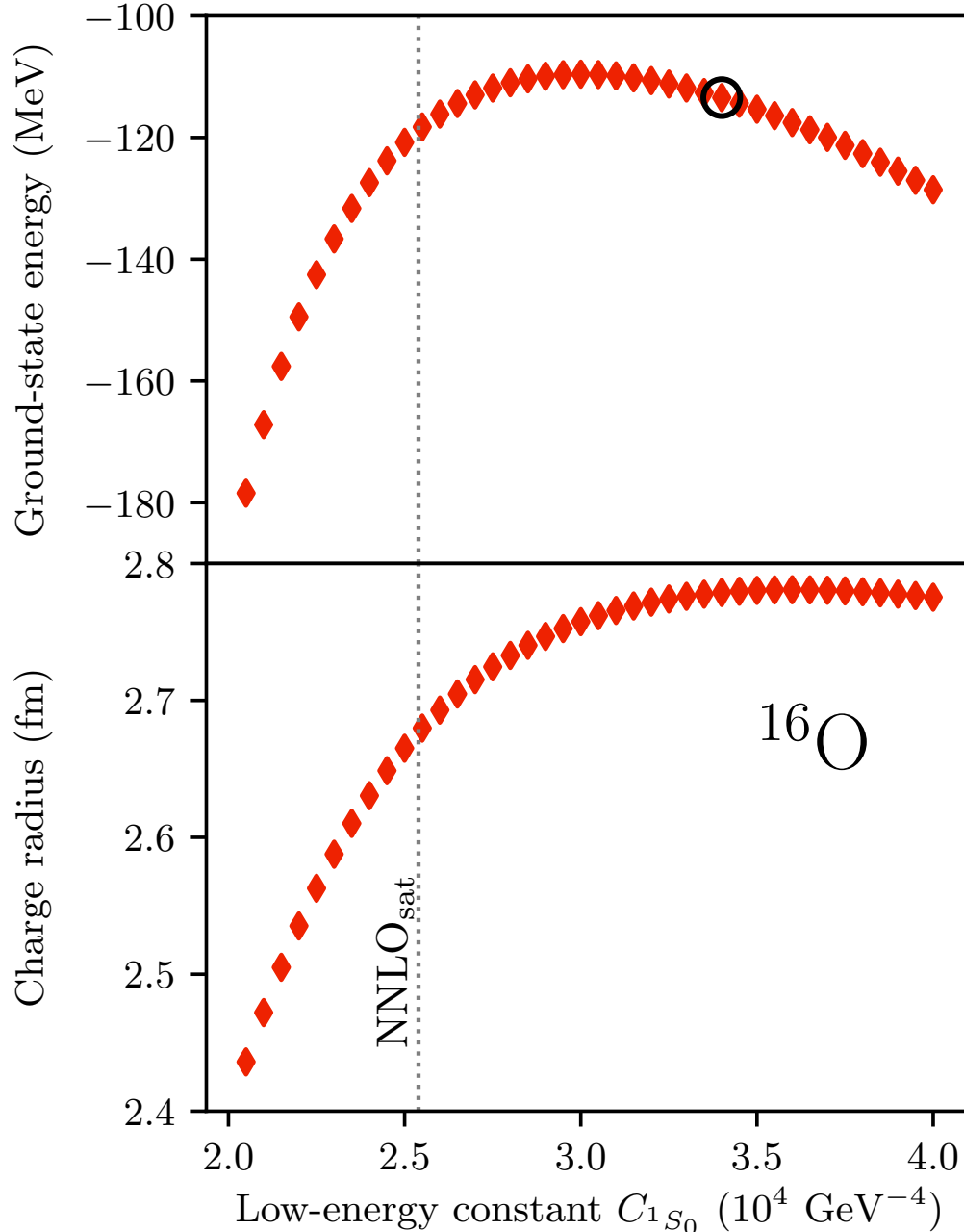
$$H(\vec{\alpha}) = \sum_{i=0}^{N_{\text{LECs}}=16} \alpha_i h_i$$

- Select “training points” where we solve exact CCSD
- Project the target Hamiltonian onto sub-space of training vectors and diagonalize the generalized eigen value problem

$$\mathbf{H}(\vec{\alpha}_\odot) \vec{c} = E(\vec{\alpha}_\odot) \mathbf{N} \vec{c},$$

Sub-space projected coupled-cluster

Andreas Ekström, Gaute Hagen PRL **123**, 252501 (2019)



- Generalization of the eigenvector continuation method [Frame D. et al., Phys. Rev. Lett. **121**, 032501 (2018)]
- Write the Hamiltonian in a linearized form

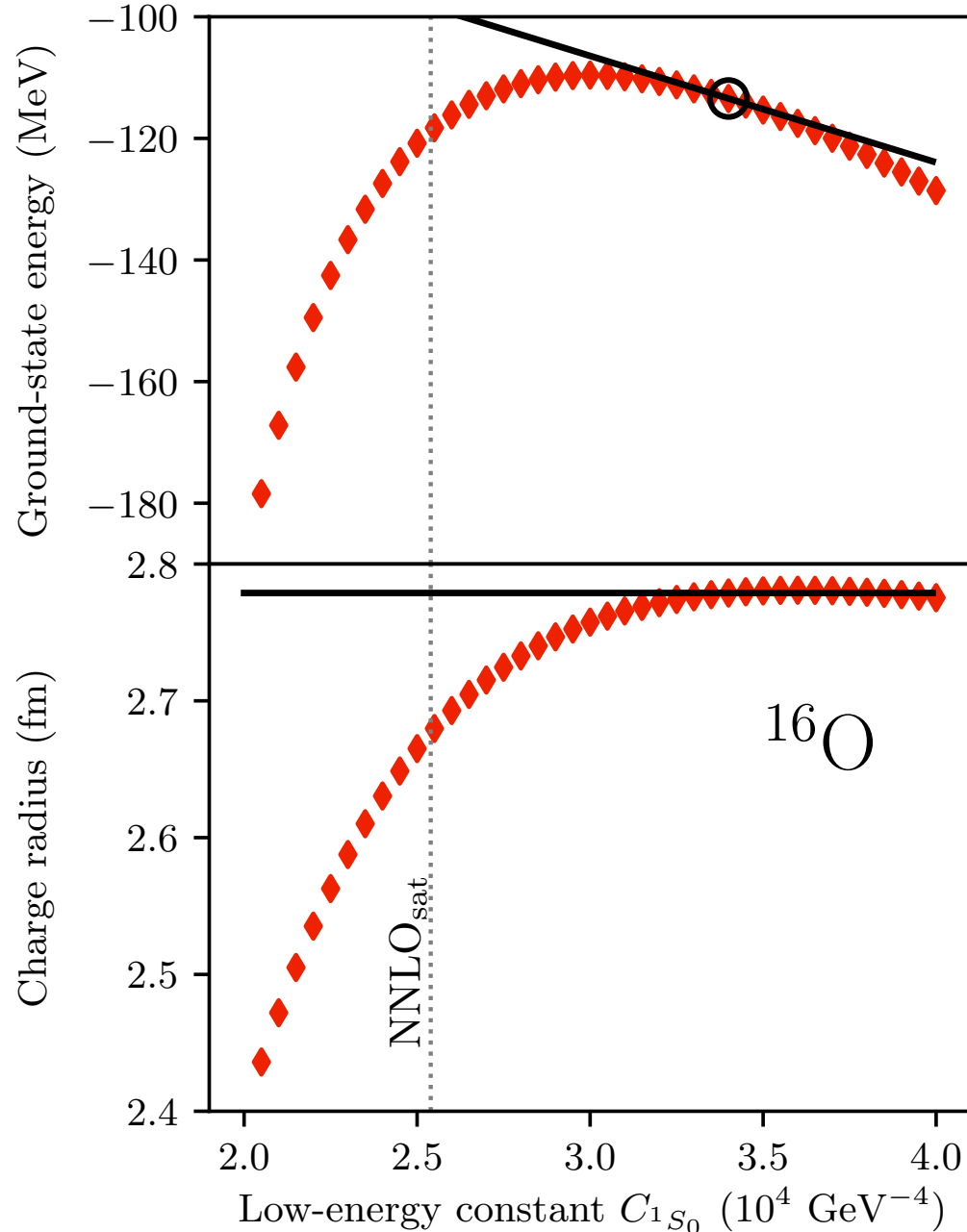
$$H(\vec{\alpha}) = \sum_{i=0}^{N_{\text{LECs}}=16} \alpha_i h_i$$

- Select “training points” where we solve exact CCSD
- Project the target Hamiltonian onto sub-space of training vectors and diagonalize the generalized eigen value problem

$$\mathbf{H}(\vec{\alpha}_\odot) \vec{c} = E(\vec{\alpha}_\odot) \mathbf{N} \vec{c},$$

Sub-space projected coupled-cluster

Andreas Ekström, Gaute Hagen PRL **123**, 252501 (2019)



- Generalization of the eigenvector continuation method [Frame D. et al., Phys. Rev. Lett. **121**, 032501 (2018)]
- Write the Hamiltonian in a linearized form

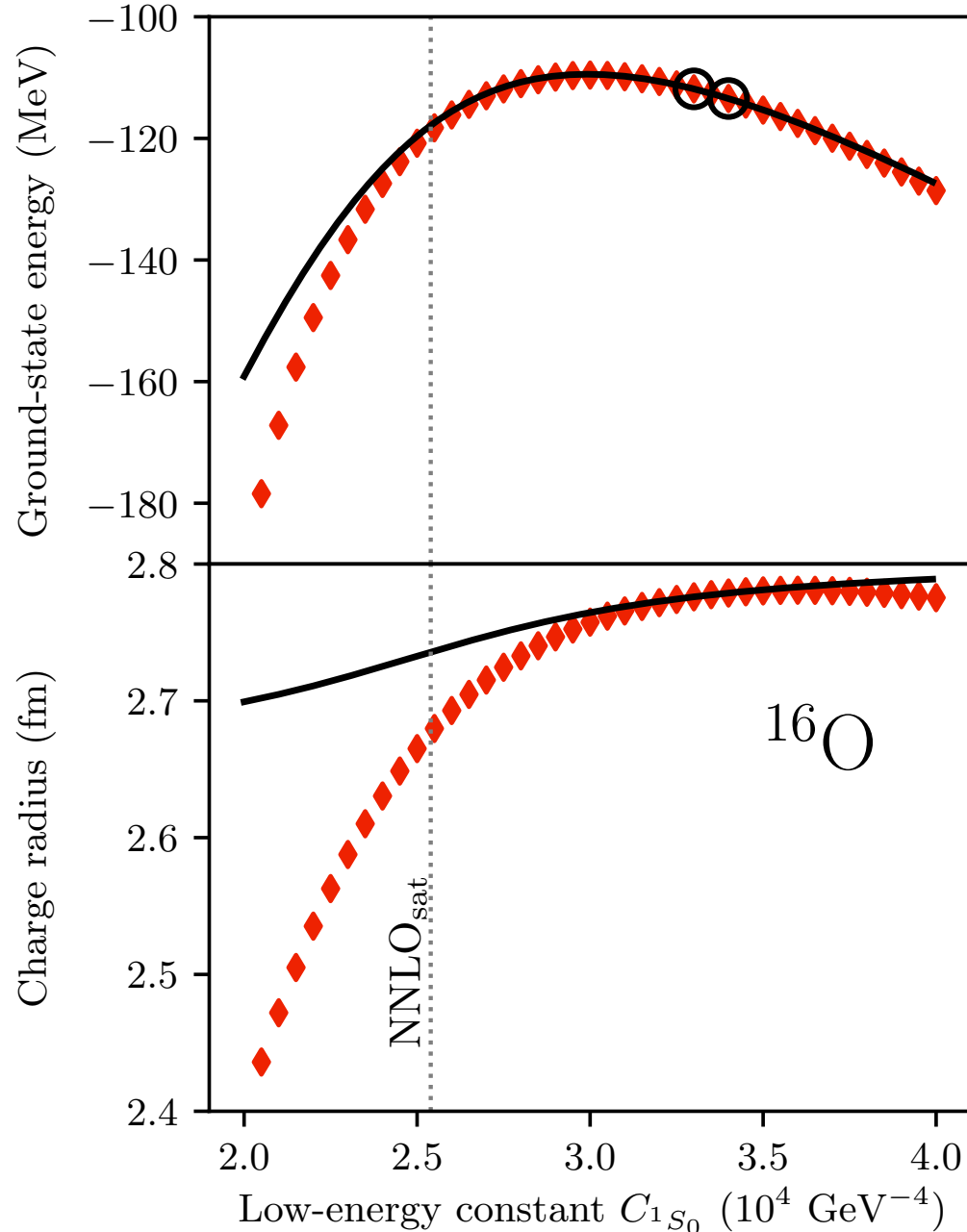
$$H(\vec{\alpha}) = \sum_{i=0}^{N_{\text{LECs}}=16} \alpha_i h_i$$

- Select “training points” where we solve exact CCSD
- Project the target Hamiltonian onto sub-space of training vectors and diagonalize the generalized eigen value problem

$$\mathbf{H}(\vec{\alpha}_\odot) \vec{c} = E(\vec{\alpha}_\odot) \mathbf{N} \vec{c},$$

Sub-space projected coupled-cluster

Andreas Ekström, Gaute Hagen PRL **123**, 252501 (2019)



- Generalization of the eigenvector continuation method [Frame D. et al., Phys. Rev. Lett. **121**, 032501 (2018)]
- Write the Hamiltonian in a linearized form

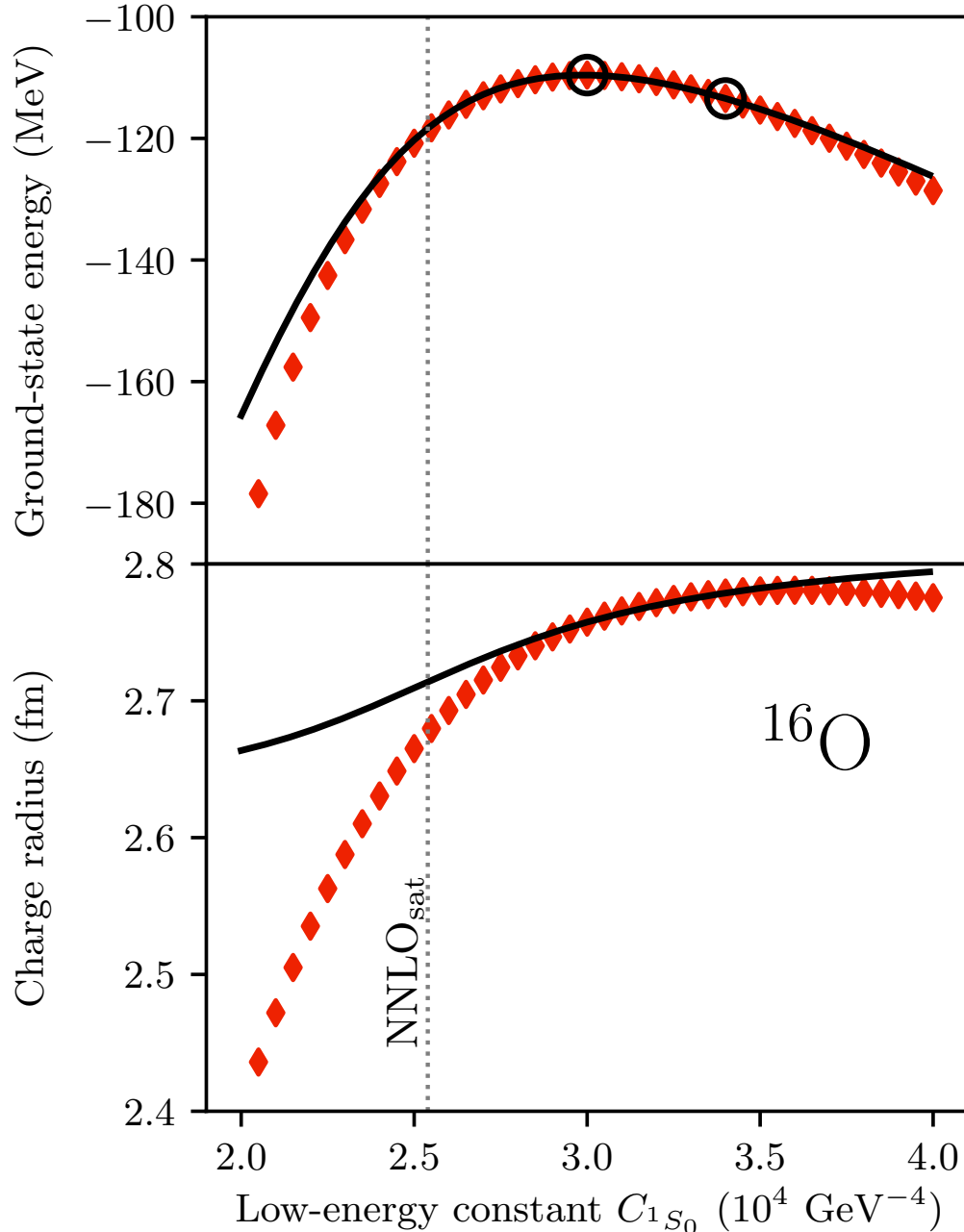
$$H(\vec{\alpha}) = \sum_{i=0}^{N_{\text{LECs}}=16} \alpha_i h_i$$

- Select “training points” where we solve exact CCSD
- Project the target Hamiltonian onto sub-space of training vectors and diagonalize the generalized eigen value problem

$$\mathbf{H}(\vec{\alpha}_\odot) \vec{c} = E(\vec{\alpha}_\odot) \mathbf{N} \vec{c},$$

Sub-space projected coupled-cluster

Andreas Ekström, Gaute Hagen PRL **123**, 252501 (2019)



- Generalization of the eigenvector continuation method [Frame D. et al., Phys. Rev. Lett. **121**, 032501 (2018)]
- Write the Hamiltonian in a linearized form

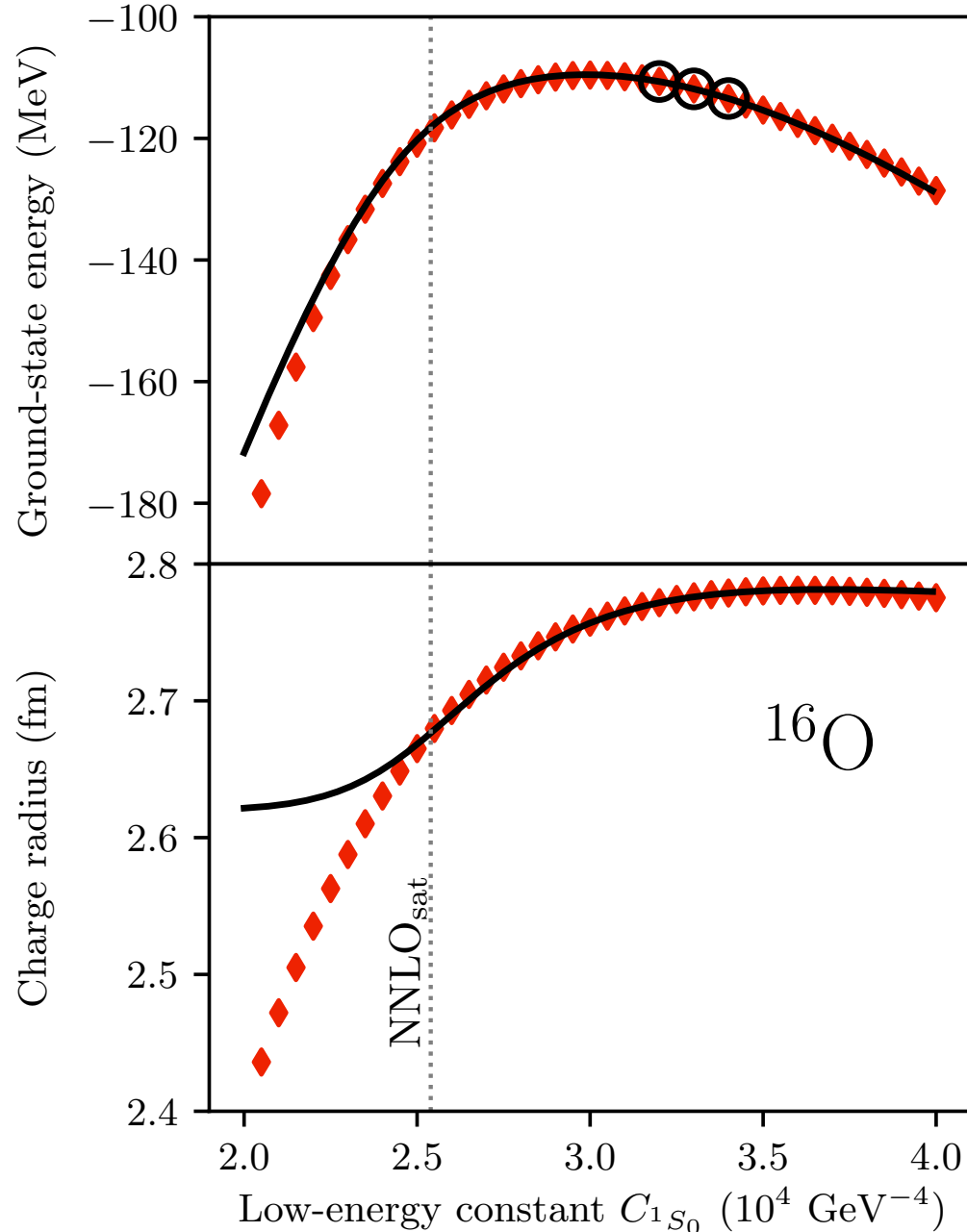
$$H(\vec{\alpha}) = \sum_{i=0}^{N_{\text{LECs}}=16} \alpha_i h_i$$

- Select “training points” where we solve exact CCSD
- Project the target Hamiltonian onto sub-space of training vectors and diagonalize the generalized eigen value problem

$$\mathbf{H}(\vec{\alpha}_\odot) \vec{c} = E(\vec{\alpha}_\odot) \mathbf{N} \vec{c},$$

Sub-space projected coupled-cluster

Andreas Ekström, Gaute Hagen PRL **123**, 252501 (2019)



- Generalization of the eigenvector continuation method [Frame D. et al., Phys. Rev. Lett. **121**, 032501 (2018)]
- Write the Hamiltonian in a linearized form

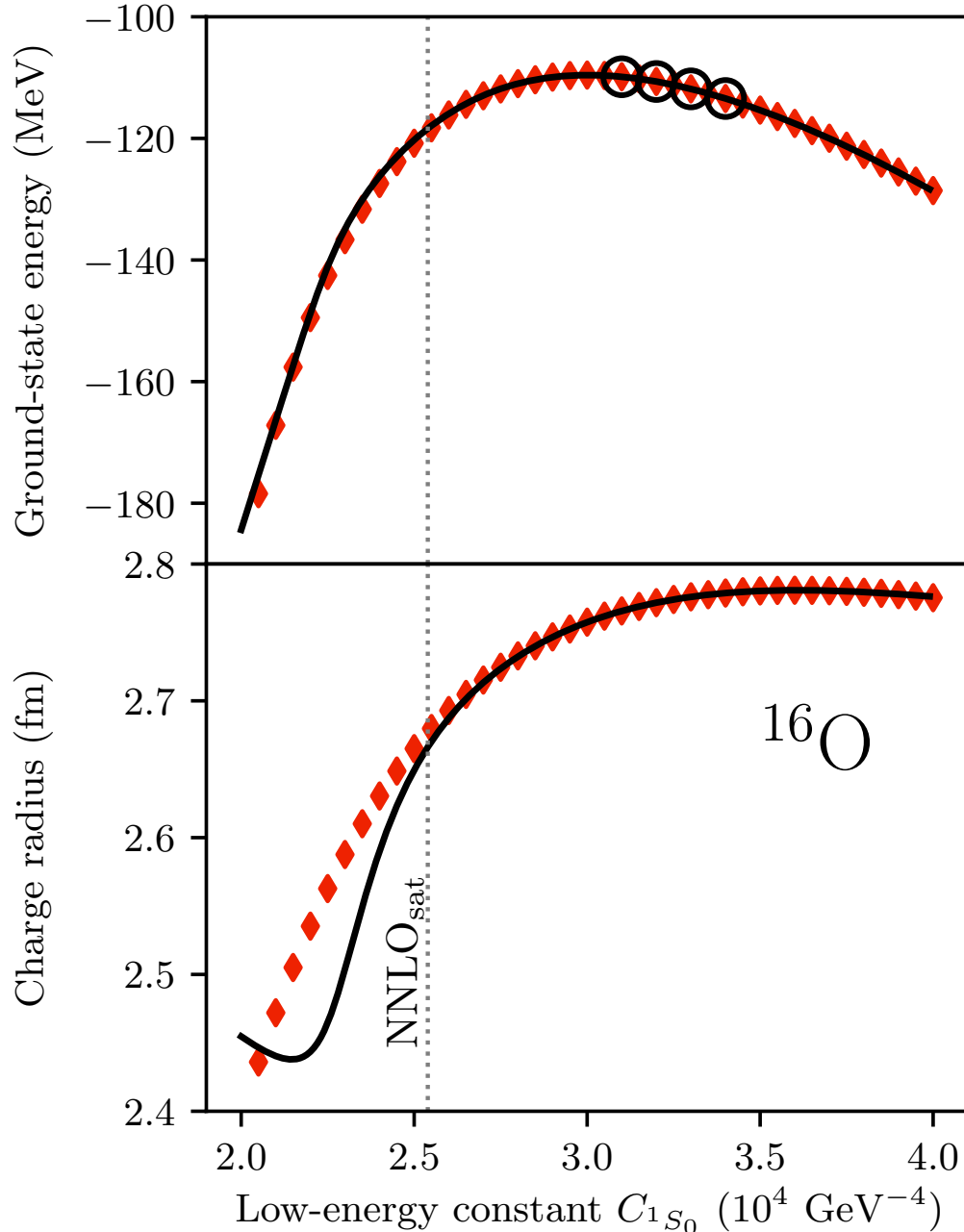
$$H(\vec{\alpha}) = \sum_{i=0}^{N_{\text{LECs}}=16} \alpha_i h_i$$

- Select “training points” where we solve exact CCSD
- Project the target Hamiltonian onto sub-space of training vectors and diagonalize the generalized eigen value problem

$$\mathbf{H}(\vec{\alpha}_\odot) \vec{c} = E(\vec{\alpha}_\odot) \mathbf{N} \vec{c},$$

Sub-space projected coupled-cluster

Andreas Ekström, Gaute Hagen PRL **123**, 252501 (2019)



- Generalization of the eigenvector continuation method [Frame D. et al., Phys. Rev. Lett. **121**, 032501 (2018)]
- Write the Hamiltonian in a linearized form

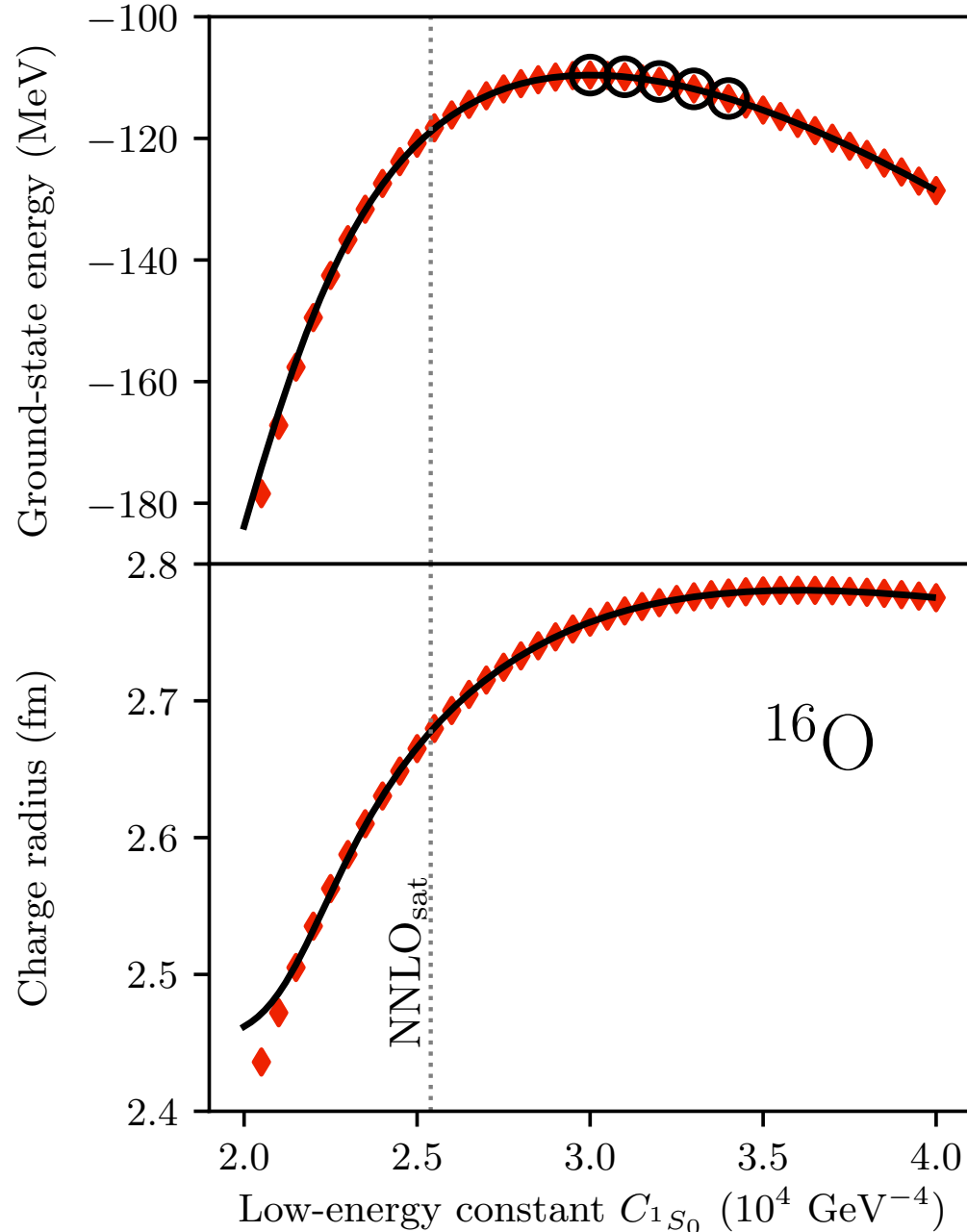
$$H(\vec{\alpha}) = \sum_{i=0}^{N_{\text{LECs}}=16} \alpha_i h_i$$

- Select “training points” where we solve exact CCSD
- Project the target Hamiltonian onto sub-space of training vectors and diagonalize the generalized eigen value problem

$$\mathbf{H}(\vec{\alpha}_\odot) \vec{c} = E(\vec{\alpha}_\odot) \mathbf{N} \vec{c},$$

Sub-space projected coupled-cluster

Andreas Ekström, Gaute Hagen PRL **123**, 252501 (2019)



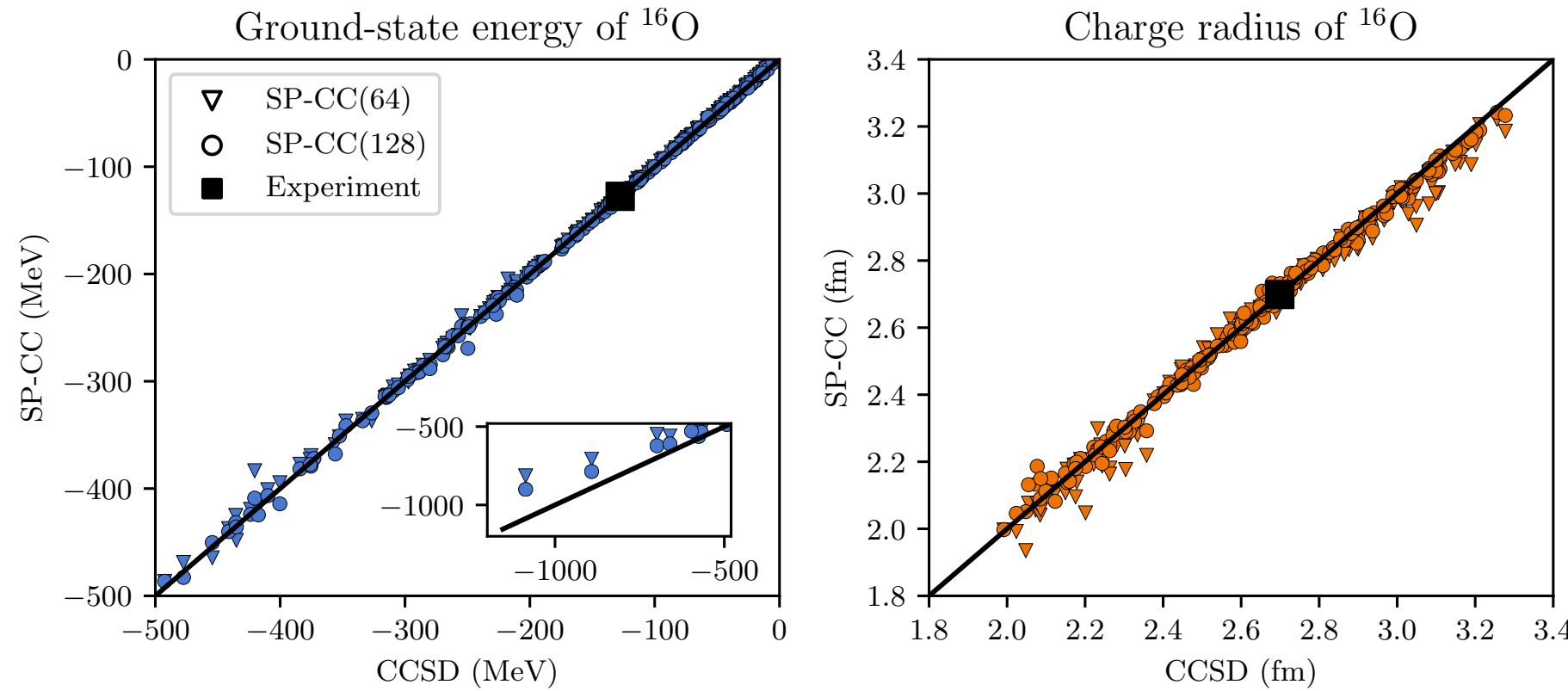
- Generalization of the eigenvector continuation method [Frame D. et al., Phys. Rev. Lett. **121**, 032501 (2018)]
- Write the Hamiltonian in a linearized form

$$H(\vec{\alpha}) = \sum_{i=0}^{N_{\text{LECs}}=16} \alpha_i h_i$$

- Select “training points” where we solve exact CCSD
- Project the target Hamiltonian onto sub-space of training vectors and diagonalize the generalized eigen value problem

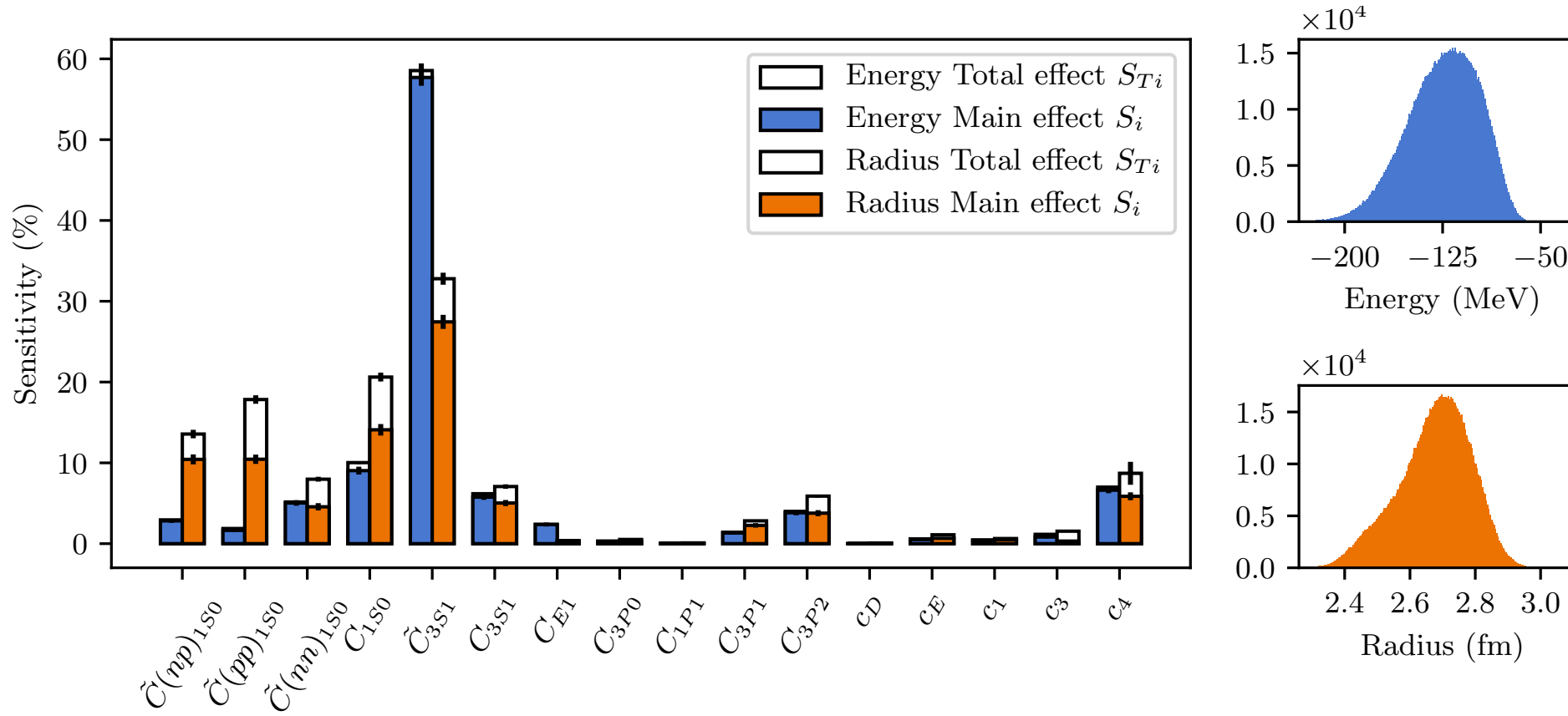
$$\mathbf{H}(\vec{\alpha}_\odot) \vec{c} = E(\vec{\alpha}_\odot) \mathbf{N} \vec{c},$$

Sub-space projected coupled-cluster – cross validation in 16 dimensions



- Select 64 and 128 sub-space vectors in the 16 dimensional space of LECs using a space-filling latin hypercube design
- Select 200 randomly exact CCSD calculations in a 20% domain around NNLO_{sat}
- With 64 subspace vectors we achieve a 1% accuracy relative to exact CCSD solutions

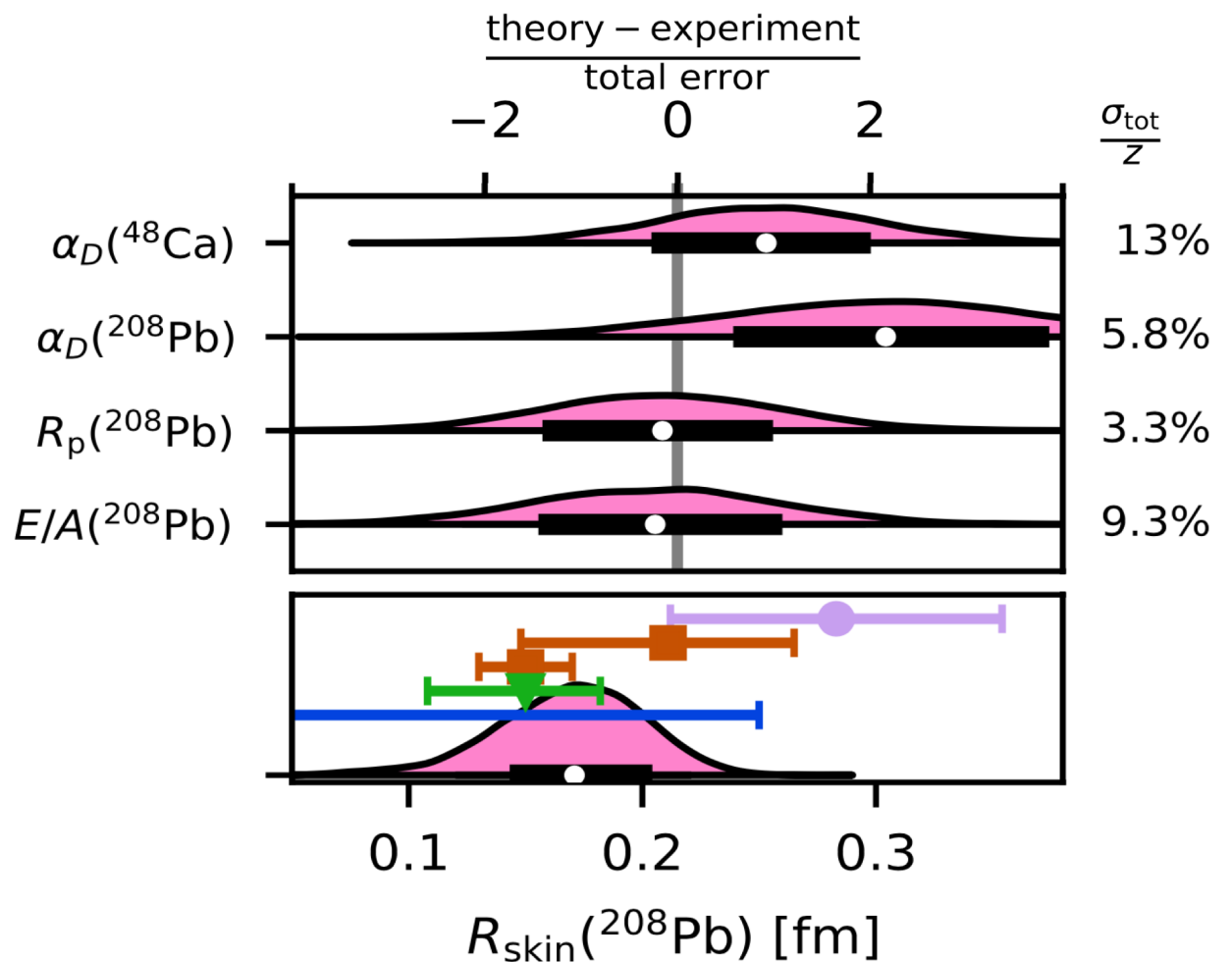
A global sensitivity analysis of the radius and binding energy of ^{16}O



- Compute the binding energy and charge radius at one million different values of the 16 LECs in one hour on a standard laptop (would require 20 years of equivalent exact CCSD computations)
- About 60% of the variance in the energy can is attributed to the $3S1$ -wave, whereas the radius depends sensitively on several LECs and their higher-order correlations

What is the neutron skin of ^{208}Pb ?

- The capability of performing billions of ab-initio simulations of selected nuclei opens up entirely new possibilities for making predictions and addressing uncertainties
- History matching – identify regions of parameter space that give results consistent with data (NN phase-shifts, $A = 2,3,4$ observables and 16-O BE and radius)

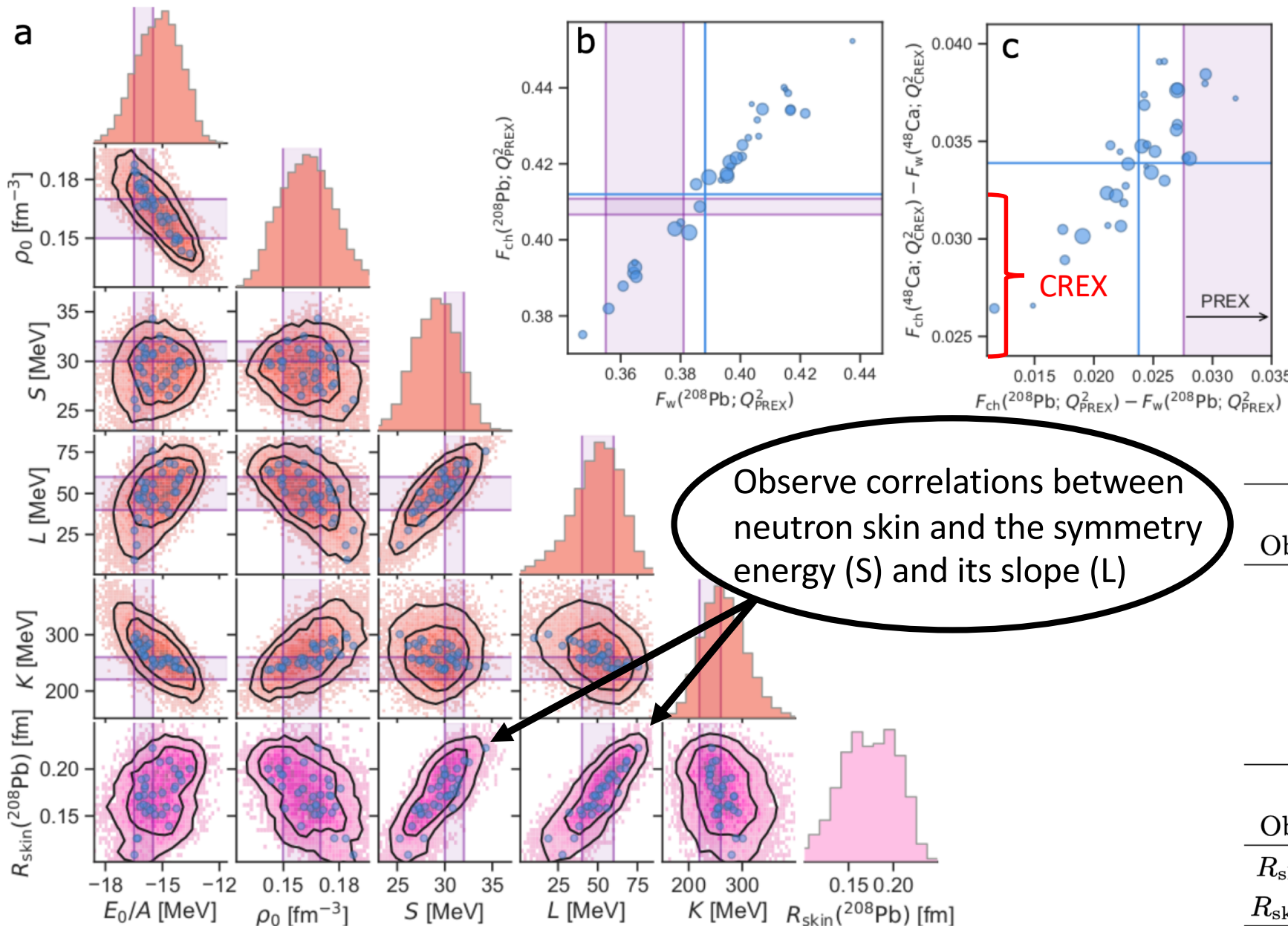


Using E/A , $E(2+)$ and R_p of Ca-48 as calibration data we are left with 34 interactions (out of 5×10^8 parametrizations)

Posterior predictive distribution for the neutron skin in ^{208}Pb compared to experiments using electroweak (purple), hadronic (red), electromagnetic (green), and gravitational waves (blue) probes.

$R_{\text{skin}}(^{208}\text{Pb}) = 0.14 - 0.20 \text{ fm}$ (68% credible interval) exhibits a mild tension with the value extracted from PREX-2

What is the neutron skin of ^{208}Pb ?

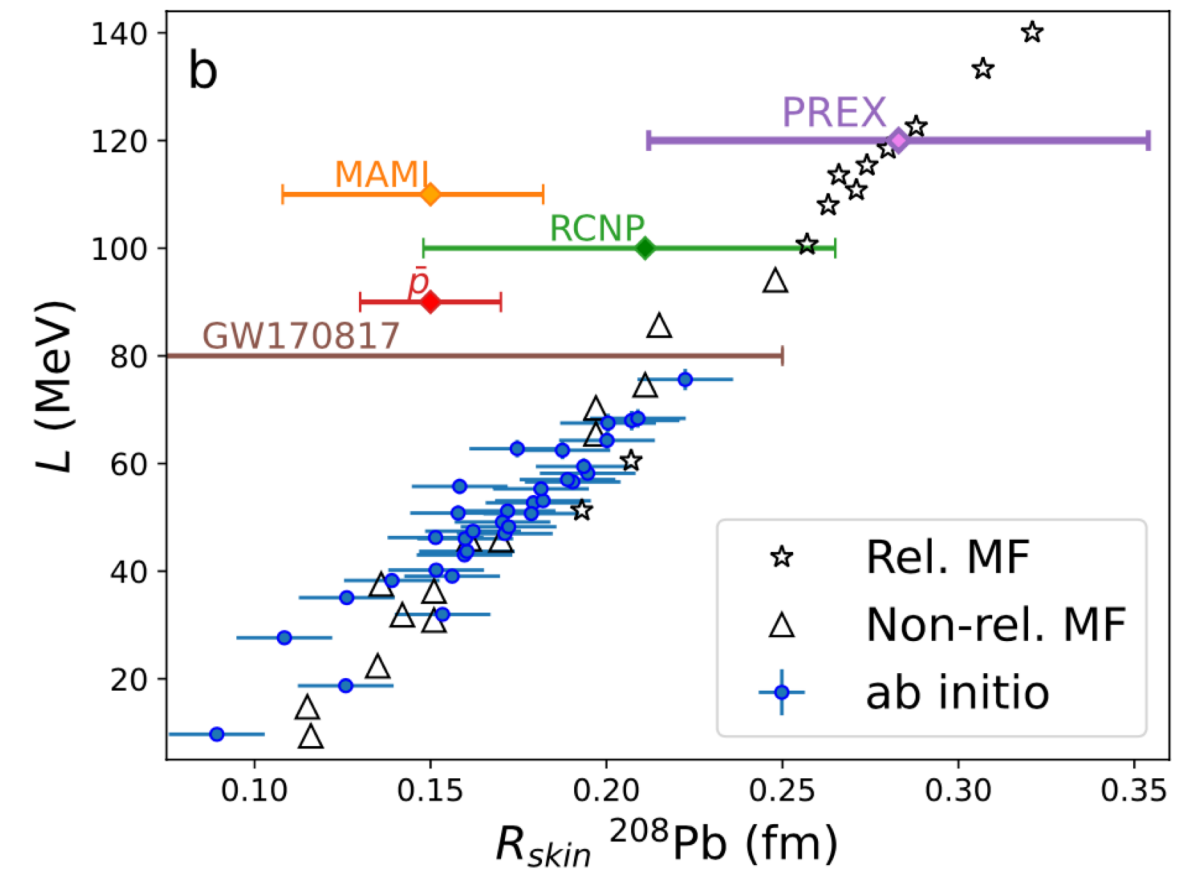
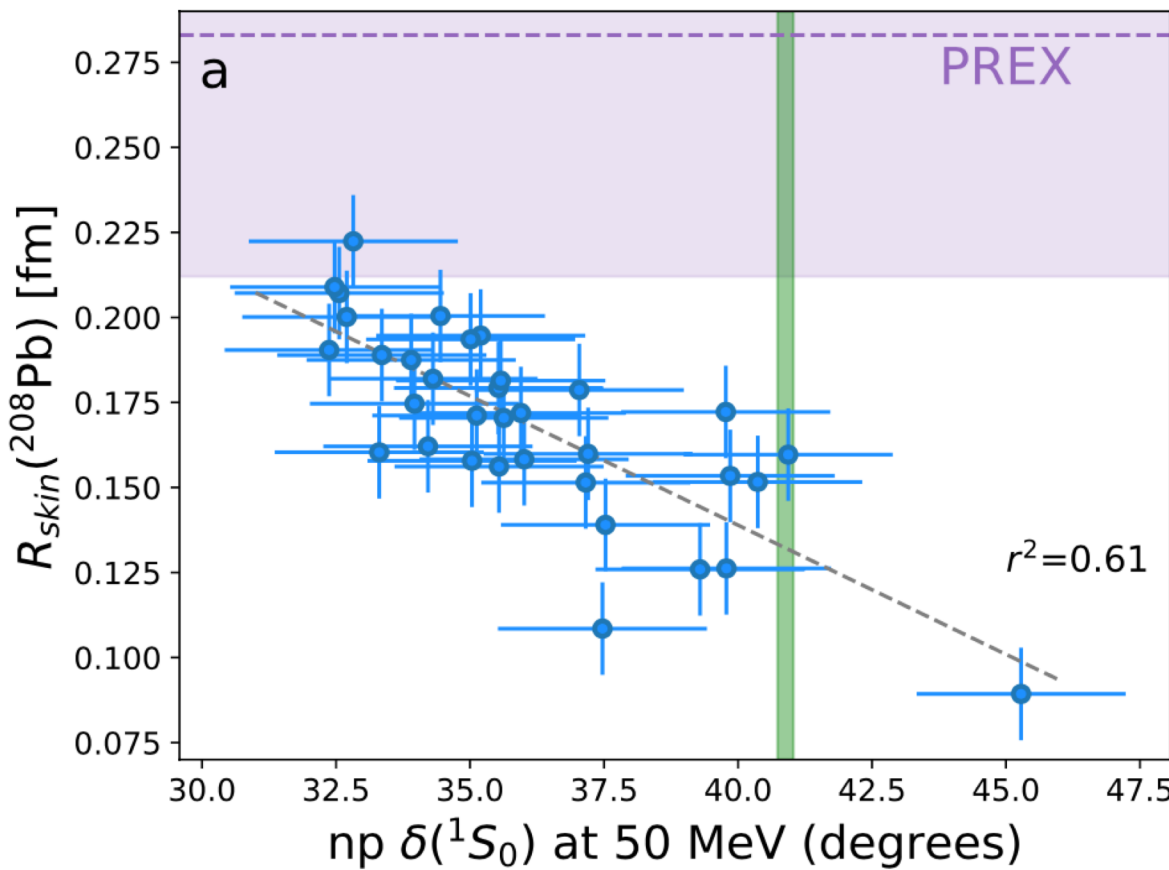


Summary of results:

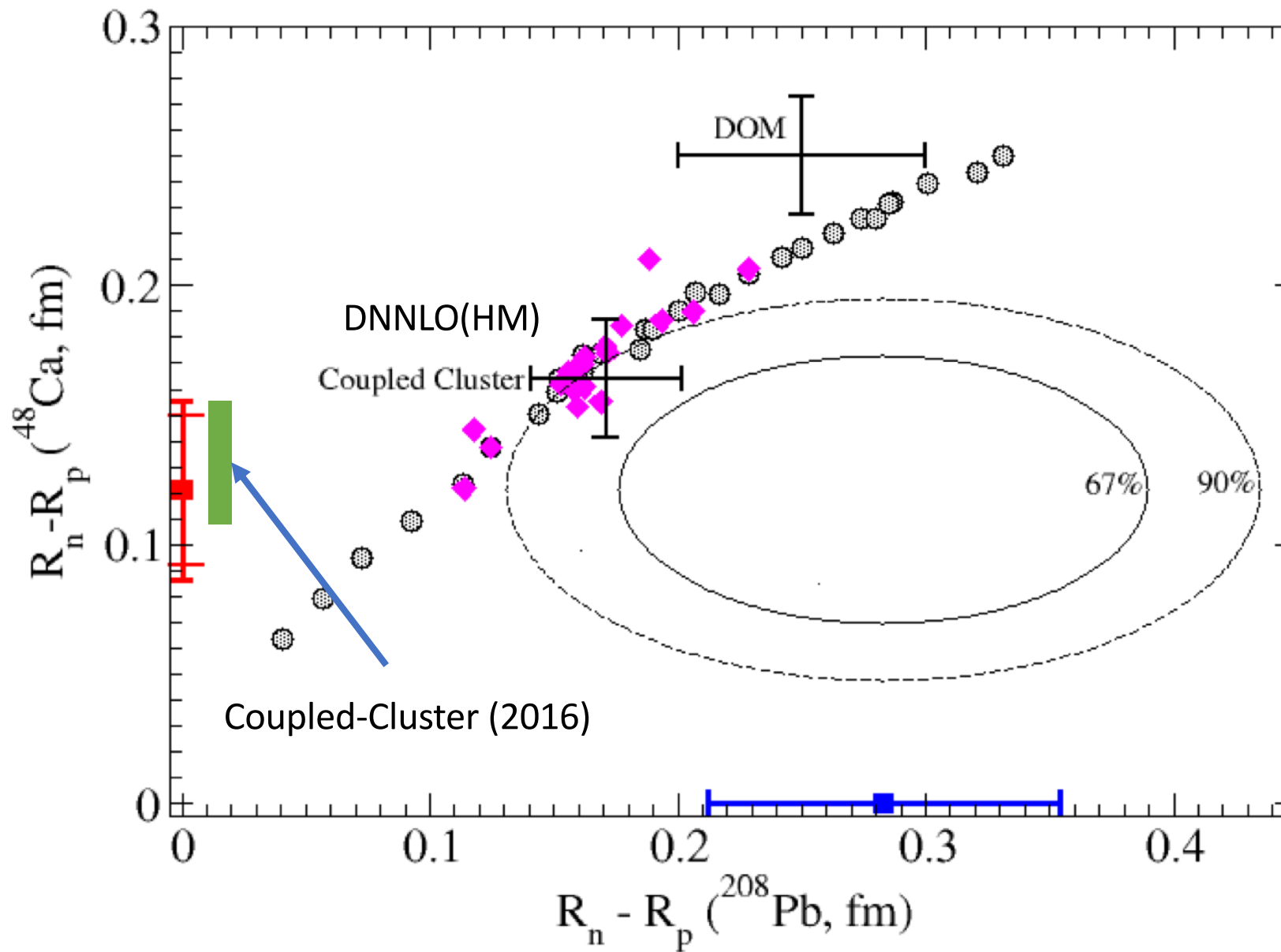
Observable	Nuclear matter properties		
	median	68% CR	90% CR
E_0/A	-15.2	[-16.3, -14.0]	[-17.2, -13.5]
ρ_0	0.163	[0.147, 0.175]	[0.140, 0.186]
S	29.1	[26.6, 31.3]	[25.132.8]
L	50.3	[37.2, 68.1]	[22.6, 75.8]
K	264	[227, 297]	[210, 328]
Neutron skins			
Observable	median	68% CR	90% CR
$R_{\text{skin}}(^{48}\text{Ca})$	0.164	[0.141, 0.187]	[0.123, 0.199]
$R_{\text{skin}}(^{208}\text{Pb})$	0.171	[0.139, 0.200]	[0.120, 0.221]

What is the neutron skin of ^{208}Pb ?

- Different models predict similar correlation between the neutron-skin and the slope of symmetry energy (L)
- The neutron skin of ^{208}Pb is (weakly) correlated with the $^1\text{S}_0$ nucleon-nucleon scattering phase-shift
- A realistic description of the $^1\text{S}_0$ scattering phase shift implies a neutron skin in tension with PREX-2



What is the neutron skin of ^{208}Pb ?



Summary

- Towards mass-table computations based on Hamiltonian methods
 - most even-even nuclei now possible with symmetry projection
 - Interactions with "good" saturation properties yield accurate description of BEs, radii and skins in light, medium-mass and heavy nuclei
 - shell closures predicted at $N = 8, 14$ in neon and magnesium and no signature of $N = 32$ shell closure in potassium
 - Universal trend of radii beyond $N = 28$ for even-even Ca-Zn isotopes
 - Odd-odd and odd-even nuclei are more challenging
 - Predicted $N = 20$ shell closure is not supported by data in isotopes of neon and magnesium
 - Steep increase in radii beyond $N = 28$ in potassium challenges theory
- Prediction of small neutron skin in ^{48}Ca confirmed by CREX
- Coherent neutrino scattering on ^{40}Ar a stepping stone for neutrino response ([see talk by Asia Sobczyk](#))

Summary

- Developed emulators that allows us to sample $\sim 10^8$ different Hamiltonians in a short time for medium mass nuclei
 - A global sensitivity analysis revealed the role of various LECs in the binding energy and radius of ^{16}O
- Combining accurate emulators, novel statistical tools, and Bayesian inference allowed us to make accurate predictions for the neutron skin and related observables in ^{208}Pb ([see talk by Weiguang Jiang](#))
- Neutron skin of ^{208}Pb in mild tension with PREX-2
- Confirmed correlations (seen in mean-field approaches) between the neutron skin of ^{208}Pb and the symmetry energy and its slope in nuclear matter



Thank you for your attention!